

**12** LEVEL III

AD-E440

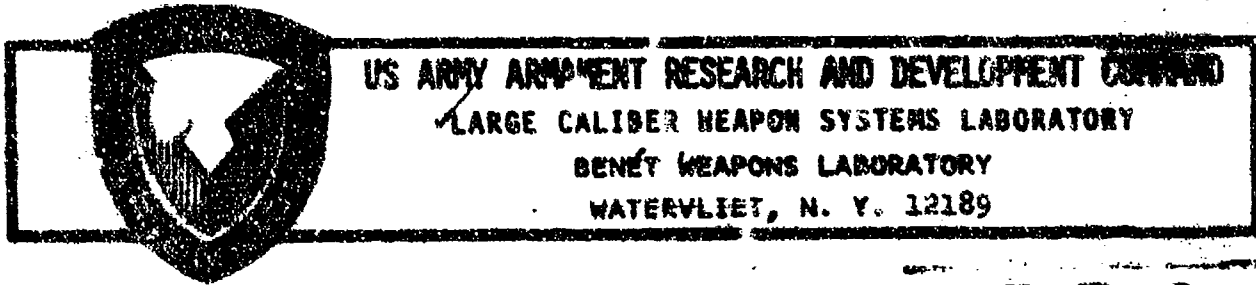
TECHNICAL REPORT ARCS-TR-78023

A069617

REFRACTORY-LINED COMPOSITE PRESSURE VESSELS

G. D'Andrea  
R. L. Cullinan  
P. J. Croteau

December 1978



AMCS No. 611101.11.84400

PRON No. M-T-51700-M7-M7

DDC  
RECEIVED  
JUN 11 1978  
REGULATED  
B

FILE COPY

APPROVED FOR PUBLIC RELEASE; DISTRIBUTION UNLIMITED

79 05 11 078

#### DISCLAIMER

The findings in this report are not to be construed as an official Department of the Army position unless so designated by other authorized documents.

The use of trade name(s) and/or manufacturer(s) does not constitute an official indorsement or approval.

#### DISPOSITION

Destroy this report when it is no longer needed. Do not return it to the originator.

REPORT DOCUMENTATION PAGE		READ INSTRUCTIONS BEFORE COMPLETING FORM	
1. REPORT NUMBER ARLCB-TR-78023	2. GOVT ACCESSION NO.	3. RECIPIENT'S CATALOG NUMBER	
4. TITLE (and Subtitle)  REFRACTORY-LINED COMPOSITE PRESSURE VESSELS		5. TYPE OF REPORT & PERIOD COVERED	
		6. PERFORMING ORG. REPORT NUMBER	
7. AUTHOR(s) G. D'Andrea R. L. Cullinan P. J. Croteau		8. CONTRACT OR GRANT NUMBER(s)	
9. PERFORMING ORGANIZATION NAME AND ADDRESS Beret Weapons Laboratory Watervliet Arsenal, Watervliet, N.Y. 12189 DRDAR-LCB-TL		10. PROGRAM ELEMENT, PROJECT, TASK AREA & WORK UNIT NUMBERS AMCMS No. 611101.11.84400 PRON No. M1-T-51700-M7-M7	
11. CONTROLLING OFFICE NAME AND ADDRESS US Army Armament Research and Development Command Large Caliber Weapon Systems Laboratory Dover, New Jersey 07801		12. REPORT DATE December 1978	
		13. NUMBER OF PAGES 80	
14. MONITORING AGENCY NAME & ADDRESS (if different from Controlling Office)		15. SECURITY CLASS. (of this report)  UNCLASSIFIED	
		15a. DECLASSIFICATION/DOWNGRADING SCHEDULE	
16. DISTRIBUTION STATEMENT (of this Report)  Approved for public release; distribution unlimited.			
17. DISTRIBUTION STATEMENT (of the abstract entered in Block 20, if different from Report)  B			
18. SUPPLEMENTARY NOTES			
19. KEY WORDS (Continue on reverse side if necessary and identify by block number) Ceramic Materials      Shrink Fitting Composite Materials      Steel Wire Filaments                  Winding Residual Stress			
20. ABSTRACT (Continue on reverse side if necessary and identify by block number) → Refractory lined pressure vessels, possessing good corrosion and erosion resistance at low and high temperatures, seem to be ideal for extending the wear life of conventional gun tubes  Since refractory materials exhibit high compressive and low tensile strength, prescribed residual stresses must be introduced to eliminate the significant			

D D C  
RECEIVED  
JUN 11 1979  
B

79 05 11 078

Continued on next page. *A*

Continued from Block 20.

tensile stresses produced during firing.

The prominent problem in fabricating such vessels is to restrict the refractory material from expanding axially during the application of the residual stresses.

This report presents manufacturing procedures to prevent the axial expansion, theoretical and experimental analyses predicting the residual and firing stress state in the vessel; and test results on 12.5 mm and 60 mm ceramic liners.

Preliminary work on 6.4 mm Tungsten-Carbon Alloy is also reported.

A

ACKNOWLEDGEMENT

The authors gratefully acknowledge the technical assistance contributed by Mr. R. Soanes of the Computer Science Section, Mr. G. Capsimalis and Dr. A. Manaker of the Physical Science Section. Special thanks to Ms. E. Fogarty for her fine typing and attitude in the preparation of this manuscript.

Accession For	
NTIS GRA&I	<input checked="" type="checkbox"/>
DDC TAB	<input type="checkbox"/>
Unannounced	<input type="checkbox"/>
Justification	
By _____	
Distribution/	
Availability Codes	
Dist	Avail and/or special
<b>A</b>	

## TABLE OF CONTENTS

	Page
ACKNOWLEDGEMENT	i
INTRODUCTION	1
TECHNICAL DISCUSSION	3
I. 12.5 mm Alumina Liner	3
II. 6.4 mm Tungsten-Carbon Alloy (CM-500) Liners	17
III. 60 mm Ceramic Liners	23
PHASE I	23
PHASE II	38
PHASE III	47
PHASE IV	58
SUMMARY	69
CONCLUSIONS	72
REFERENCES	74

## ILLUSTRATIONS

1. Stresses developed in 12.5 mm alumina specimens (30 Ksi T.S.)	4
2. Stresses developed in 12.5 mm alumina specimens (0 Ksi T.S.)	5
3. Diametrical change vs layers for 12.5 mm alumina specimens	6
4. Dimensional and physical properties of 12.5 mm alumina specimens	8
5. Fixturing used in winding along with 4 finished specimens	9
6. Diametrical change vs layers wound at 4 lb/end tension	11
7. Diametrical change vs layers wound at 4 lb/end tension	12
8. Pressure-strain data for typical 12.5 mm alumina liners	15
9. Stresses developed in 6.4 mm W-C alloy specimens (155 Ksi T.S.)	19

	<u>Page</u>
10. Stresses developed in 6.4 mm W-C alloy specimens (0 Ksi T.S.)	20
11. Diametrical change vs layers for 6.4 mm W-C specimens	21
12. Sketch of 60 mm alumina specimens	24
13. View of 60 mm specimens from Phase I	31
14. Diametrical change vs layers for specimen 60-1	32
15. Diametrical change vs layers for specimen 60-2	33
16. Stresses developed in specimen 60-2 with a 30 Ksi T.S.	34
17. Stresses developed in specimen 60-2 with a 0 Ksi T.S.	35
18. Hoop strain vs. wound layers of specimen 60-2	36
19. Longitudinal strain vs wound layers of specimen 60-2	37
20. View of finished specimen 60-3 used in Phase II	43
21. Stresses developed in specimen 60-3 with a 30 Ksi T.S.	44
22. Stresses developed in specimen 60-3 with a 0 Ksi T.S.	45
23. Diametrical change vs wound layers of specimen 60-3	46
24. Specimens 60-6, -7, and -8 from Phase III	54
25. Schematic showing action of friction forces	59
26. Radial stress distribution caused by .002" interference fit	61
27. Tangential stress distribution caused by .002" interference fit	62
28. Radial stress distribution caused by 12 Ksi internal pressure	63
29. Tangential stress distribution caused by 12 Ksi internal pressure	64
30. Maximum compressive pressure vs alumina wall ratio	71

TABLES

	Page
1. INTERNAL STRAIN DATA ON 12.5 MM ALUMINA SPECIMENS	10
2. DESIGN AND TEST DATA ON 12.5 MM ALUMINA SPECIMENS	13
3. DETAILS OF THE TUNGSTEN-CARBON SPECIMEN	18
4. CALIBRATION DATA ON THE 100 KSI LOAD CELL	22
5. INTERNAL STRAIN DATA OF SPECIMEN 60-1	26
6. INTERNAL STRAIN DATA OF SPECIMEN 60-2	28
7. INTERNAL STRAIN DATA OF SPECIMEN 60-3	39
8. LONGITUDINAL STRAIN VS TORQUE APPLIED TO SPECIMEN 60-3	40
9. SHRINK-FITTING STRAINS INDUCED IN 60 MM ALUMINA CYLINDER	49
10. INTERNAL STRAIN DATA DURING FABRICATION OF SPECIMEN 60-6	49
11. INSIDE DIAMETER PROFILE OF SPECIMEN 60-7 BEFORE AND AFTER SHRINK-FITTING	52
12. INSIDE DIAMETER PROFILE OF SPECIMEN 60-8 BEFORE AND AFTER SHRINK-FITTING	56
13. INTERNAL STRAIN DATA FROM THE WINDING OF SPECIMEN 60-8	57
14. COMPUTER PRINTOUT DATA ON SIMULTANEOUS LINER/JACKET YIELDING (SHFUTMP)	66

## INTRODUCTION

An ideal material for the bore of cannon tubes is one which exhibits high strength, moderate ductility, high hardness, good corrosion and erosion resistance at low and high temperatures. The lack of this "super" material in present-day ordnance introduces weapons with reduced efficiency and effectiveness. As a result, trade offs are made with respect to rate of fire, projectile mass and velocity, gun barrel life, etc. To correct some of these deficiencies, the Benet Weapons Laboratory has conducted limited studies in replacing all or part of the steel in the gun barrels with those made from refractory materials. These liners were placed under compressive residual stresses by shrink fitting them into metallic jackets and/or the high tension winding of high strength filaments in suitable binders on the liners. Similar work was proposed<sup>1</sup> in the past.

Refractory-lined cannon barrels offer the potential of:

- a. Increased corrosion and erosion resistance.
- b. Increased rates of fire. Refractory liners with low thermal conductivity and heat capacity per unit volume will allow a greater number of rounds to be fired before the barrel temperature would become excessive.

<sup>1</sup>L. A. Behrman, et al., "Feasibility of Refractory-Lined Composite Gun Barrels," Physics International Co. Report No. PIIR-11-72, Feb. 1972.

c. Potential overall increased performance efficiency. In conventional steel guns, approximately 20% of propellant energy is lost in heat to the barrel and projectile; with a refractory liner this will be minimized, and a significant amount of this "lost energy" could be retained.

This report briefly analyzes the following system configurations and draws conclusions on their merits and disadvantages:

1. 12.5 mm ceramic liner wound with high strength steel filaments.
2. 6.4 mm tungsten-carbon (CVD) alloy wound with high strength steel filaments.
3. 60 mm ceramic liners:
  - (a) Wound with steel filaments.
  - (b) Shrink fitted into a metallic jacket and later wound.
  - (c) Shrink fitted into a gun steel jacket.

Configurations (1), (2), (3a), and (3b) have been theoretically analyzed with computer program TENZAU<sup>2</sup>, while configuration (3c) has been analyzed with computer program SHFUTMP (shrink fit uniform temperature).

---

<sup>2</sup>G. D'Andrea and R. Cullinan, "Application of Filament Winding to Cannon and Cannon Components. Part III: Summary Report," Watervliet Arsenal Technical Report WVT-TR-76035, October 1976.

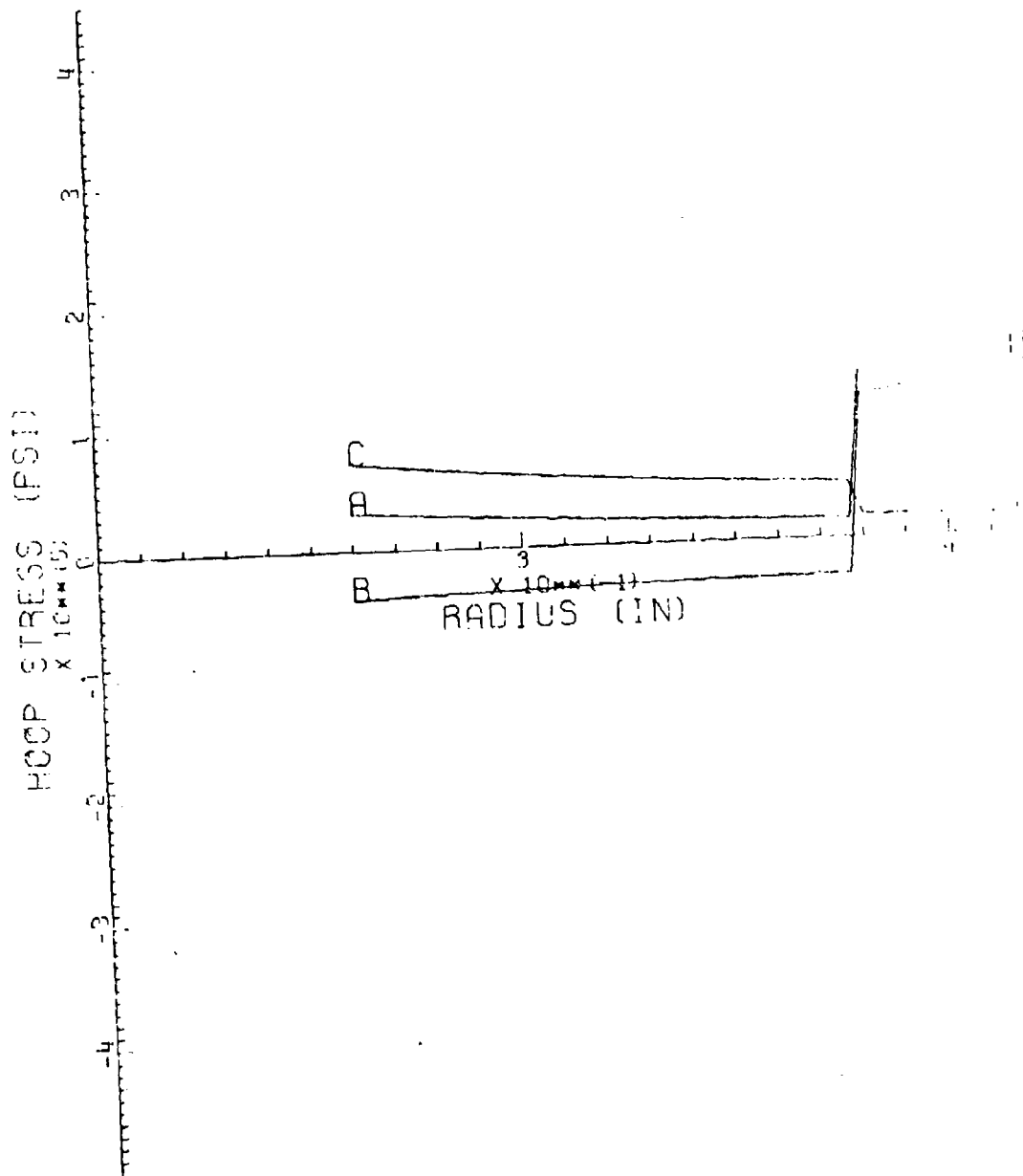
In all of the experimental work, the composite jackets were made of 6 mil N-S 355 (S.S.) wire with a minimum tensile strength of 450 Ksi. An anhydride cured epoxy formulation was used as the binder. The volume ratio of filament/binder was 70% and the cure cycle calls for a gelling stage of 1 hour at 200°F with final cure being 2 hours at 350°F.

#### TECHNICAL DISCUSSION

##### I. 12.5 mm Alumina Liner

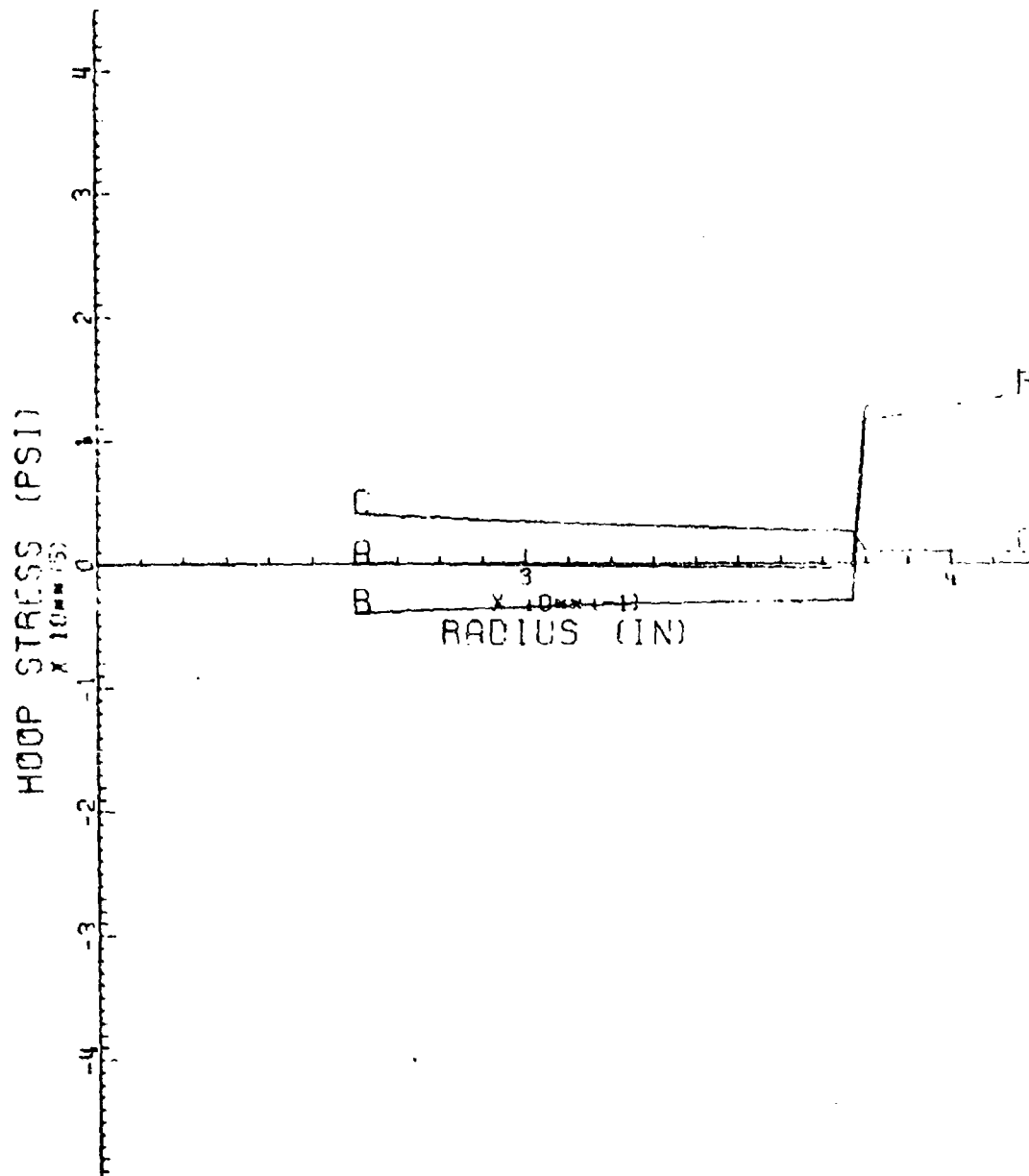
A typical theoretical analysis obtained from TENZAUTO is shown in Figures 1, 2, and 3. Figures 1 and 2 show the expected residual stress (curve B-B) as introduced by the filament winding process. The service stress, A-A of Figure 1, produced by an internal pressure of 27.5 Ksi, considers a 30,000 Psi rupture strength for the ceramic. Figure 2 considers the ceramic liner to have no tensile strength hence a reduction in the theoretical pressure capacity, i.e., 15.8 Ksi. This assumption is considered to be a must for the proper design of such composites because it prevents micro-cracks from forming since the ceramic is not under tension during the service cycle. This adds an additional factor of safety to the component.

Figure 3 represents the theoretical results of the diametrical change of the liner as a function of the number of layers. This last output is very important since it allows the filament winding operator to monitor the theoretical results as the component is being fabricated.



(PRESSURE = 27480 PSI)  
 SERVICE = A-A, RESIDUAL = B-B, ELASTIC = C-C

Figure 1. Stresses developed in 12.5 mm alumina specimens (30 Ksi T.S.)



(PRESSURE = 15765 PSI)  
 SERVICE = A-A, RESIDUAL = B-B, ELASTIC = C-C

Figure 2. Stresses developed in 12.5 mm alumina specimens (0 Ksi T.S.)

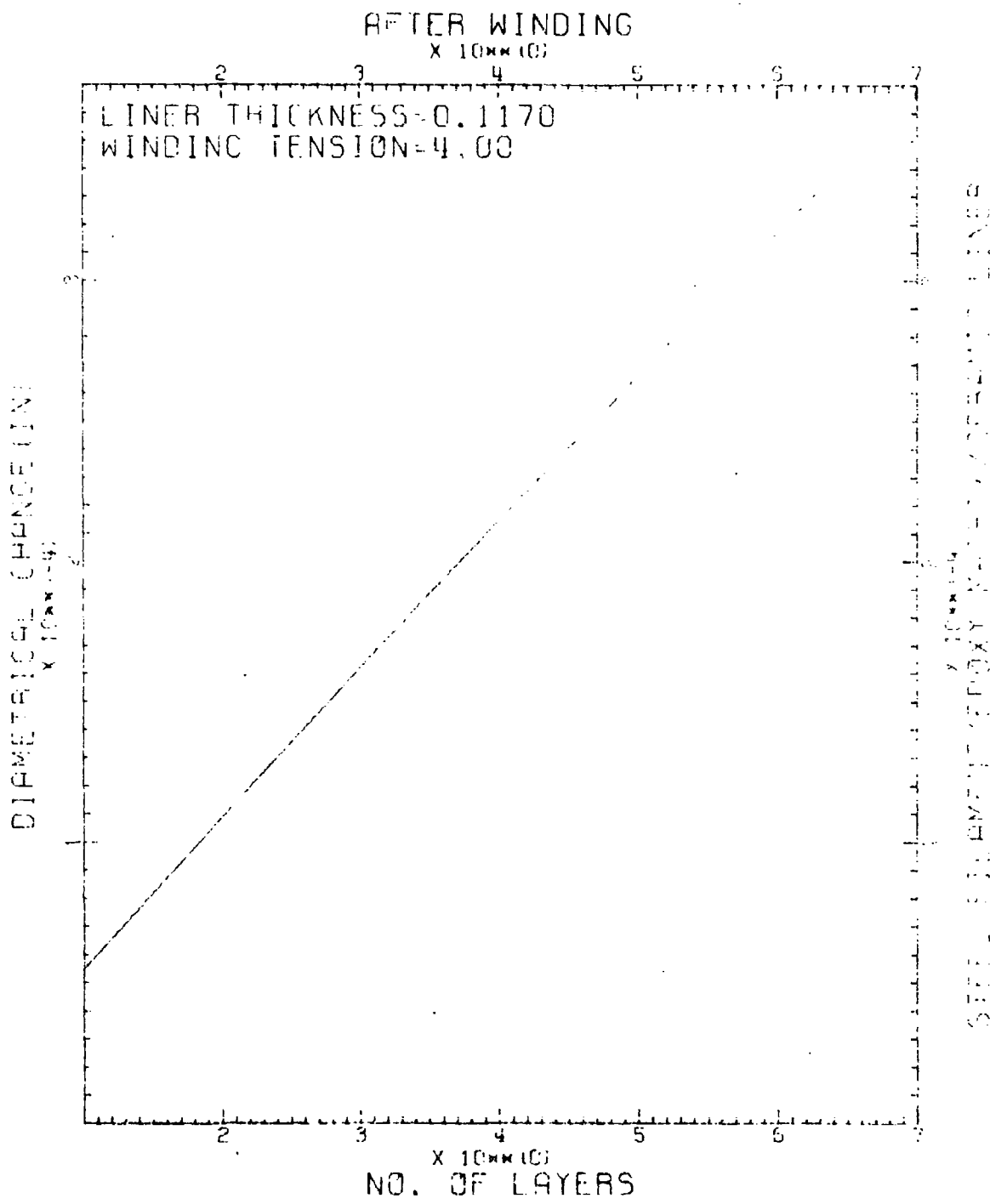


Figure 3. Diametrical change vs layers for 12.5 mm alumina specimens

## FABRICATION

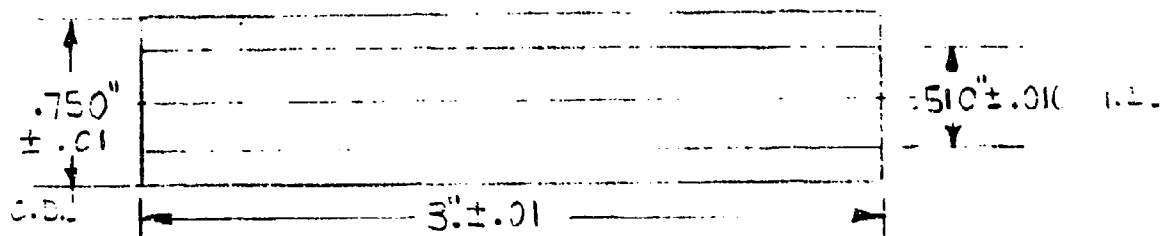
First attempts at experimental work to verify the theory involved the use of small diameter Alumina tubing as liners. These liners were made of high grade Alumina (99.8%) with the dimensions and properties shown in Figure 4.

Fixturing was made to allow for holding the liners during the winding operation and is shown in Figure 5 along with some of the specimens.

Before the actual winding of the composite jackets, a brief dry run test was performed to correlate the theoretical output of TENZAUTO. A hoop strain gage was centrally mounted inside one of the Alumina cylinders. This was done so that the compressive hoop strain (and corresponding deflection) generated by each hoop layer could be measured. Table 1 shows the strain data from winding 11 layers at 4 lb/end tension and 15 layers at 6 lb/end tension. In both cases, strain was recorded after every layer during winding. The cylinder was held under tension overnight and the following day the strain was recorded again.

Figures 6 and 7 show the theoretical curves for each winding condition as determined by TENZAUTO along with the actual data points recorded during this test.

Eight test samples were fabricated for eventual burst testing. Table 2 shows the fabrication make-up of each cylinder (SN-5 was inadvertently cracked during fabrication). The steel wire that was used was the aforementioned 6 mil S.S. wire. The winding tension of the wire was 4 lb/end and the hoop coverage per layer averaged 162 ends/inch.



MATERIAL	998*	
CONSTITUTION	99.8% Al <sub>2</sub> O <sub>3</sub>	
BULK SPECIFIC GRAVITY	3.85	
FLEXURAL STRENGTH (KSI)	55	
COMPRESSIVE STRENGTH (KSI)	>300	
TENSILE STRENGTH (KSI)	30	
YOUNG'S MODULUS x 10 <sup>6</sup> psi	57	
MAX. WORKING TEMP. (°C)	1950	
THERM. CONDUCT.	24°C	230
BTU/ft. <sup>2</sup> hr. °F/in.	800°C	60
THERMAL EXPANSION	24-250°C	6.2
per °C	24-500°C	7.4
x 10 <sup>-6</sup>	24-1000°C	8.5
	24-1500°C	9.8

\* M<sup>C</sup>DANIEL CO.  
CHALFOUNT, PA

Figure 4. Dimensional and physical properties of 12.5 mm alumina specimens

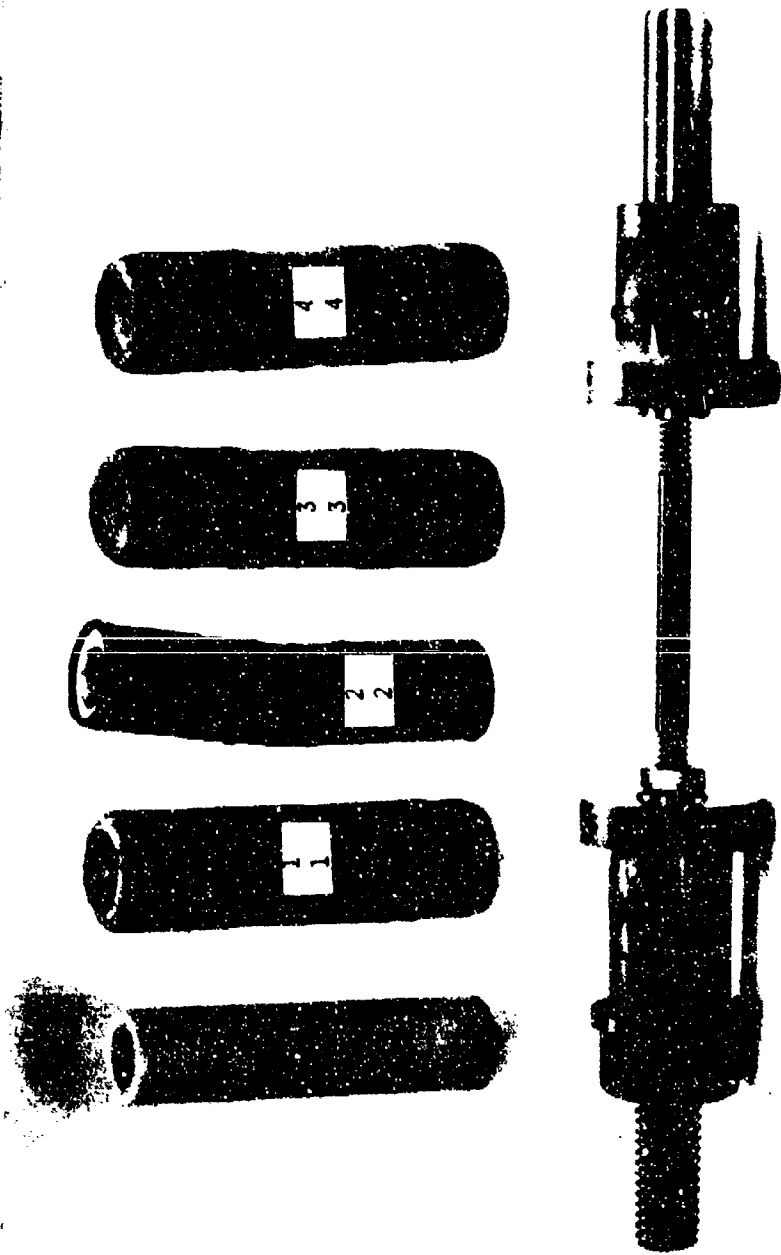


Figure 5. Fixturing used in winding along with 4 finished specimens

TABLE 1. INTERNAL STRAIN DATA ON 12.5 MM ALUMINA SPECIMENS (DRY RUN)

No. of Layers	Tension = 4 lb/end Coverage = 163 ends/in		Tension = 6 lb/end Coverage = 163 ends/in	
	$\epsilon_H$ ( $\mu\text{in/in}$ )	$\Delta D$ (in)	$\epsilon_H$ ( $\mu\text{in/in}$ )	$\Delta D$ (in)
0	0	.00004	0	.00009
1	-75		-175	
2	-175		-335	
3	-295		-465	
4	-385		-600	
5	-475		-710	
6	-545	.00028	-830	.00043
7	-610		-970	
8	-685		-1080	
9	-775		-1205	
10	-830		-1320	
11	-915	.00048	-1410	.00073
12			-1500	
13			-1595	
14			-1690	
15			-1790	.00093
Overnight	-900		-1770	

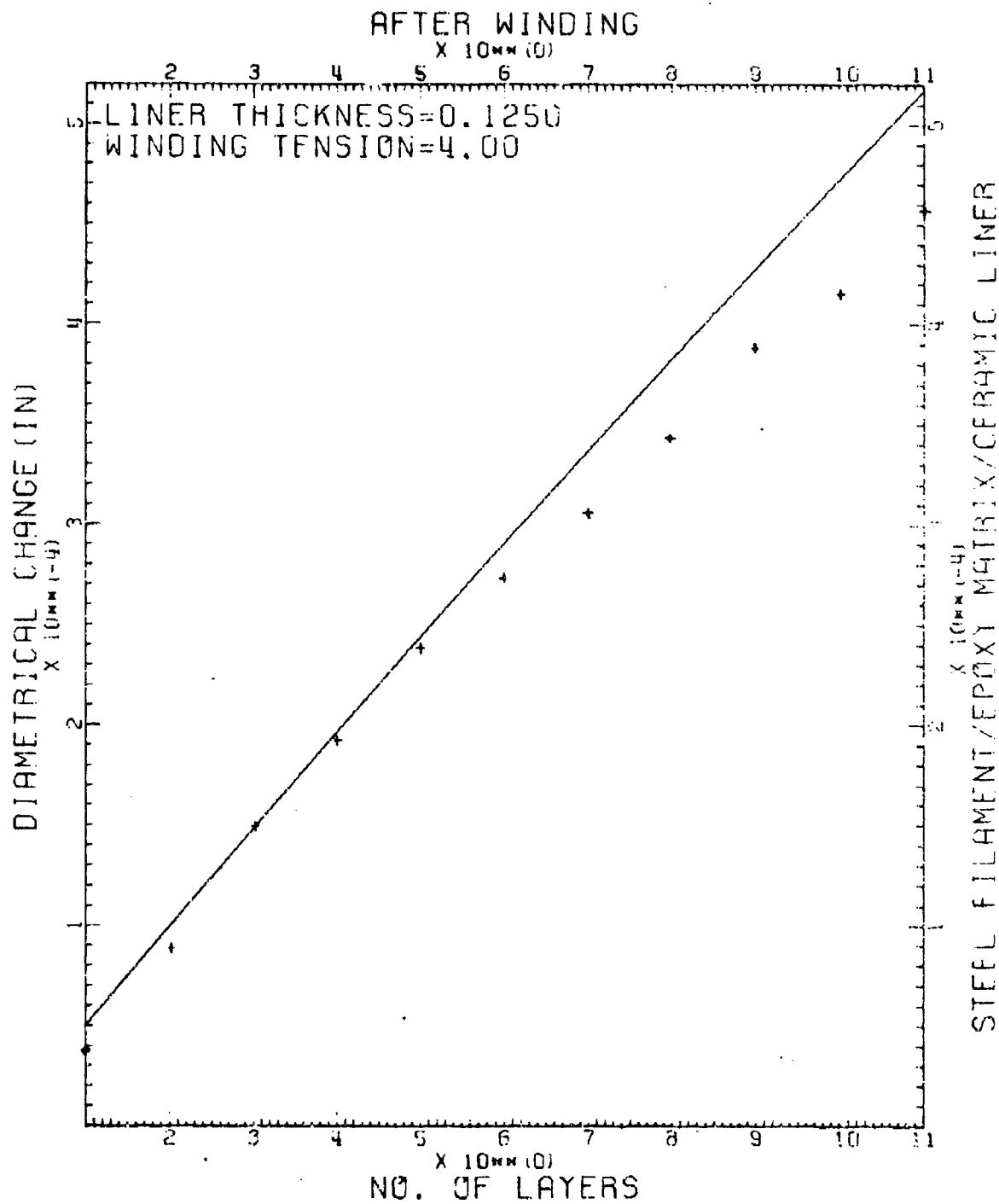


Figure 6. Diametrical change vs layers wound at 4 lb/end tension

AFTER WINDING  
X 10<sup>mm</sup> (1)

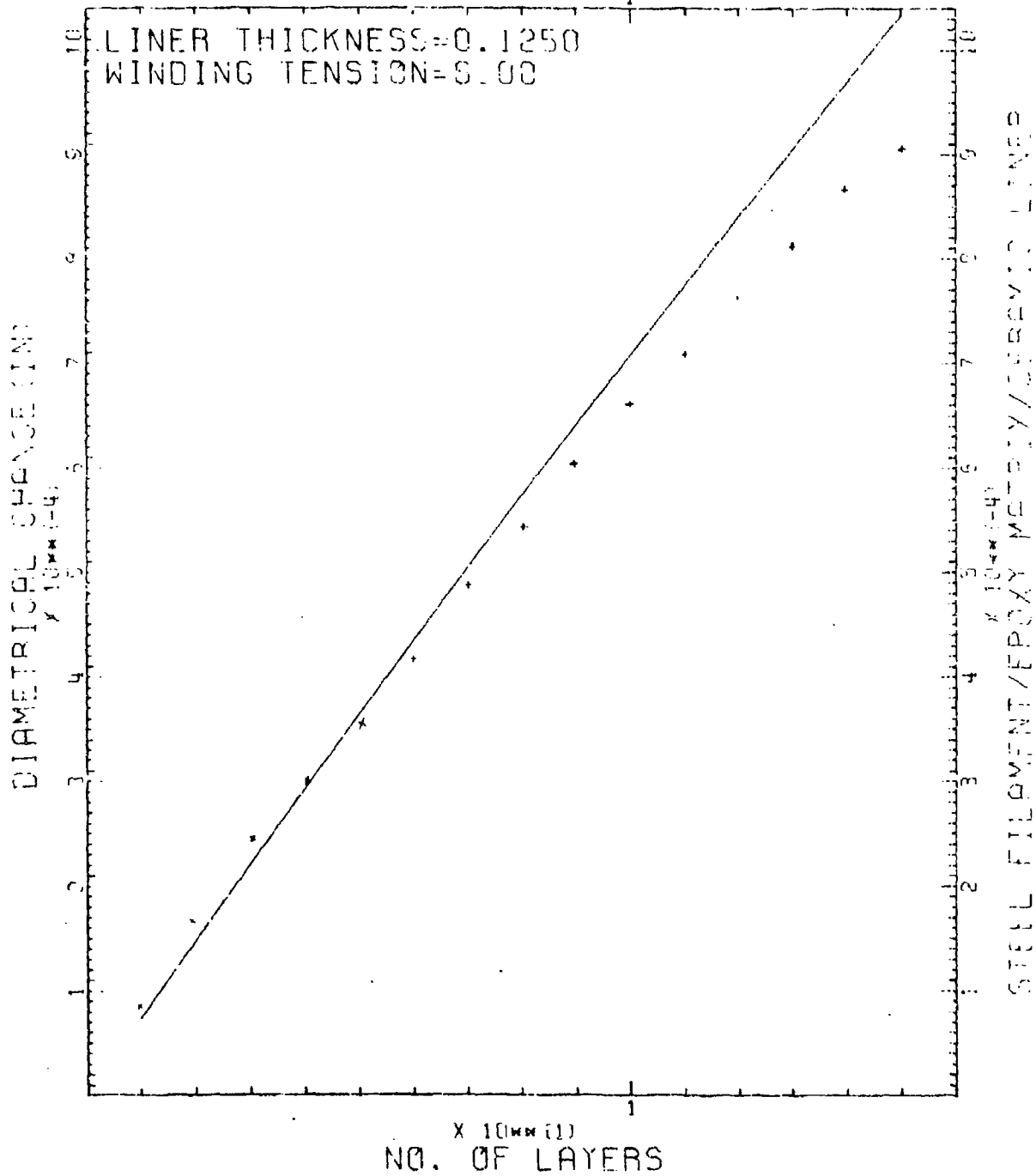


Figure 7. Diametrical change vs layers wound at 4 lb/end tension

TABLE 2. DESIGN AND TEST DATA ON 12.5 MM ALUMINA SPECIMENS

S/N	Layers	Burst Press.	Theory (Ksi)	
			*	**
- 1	A. 10 Hoops Wire (Gelled) B. 2 Hcls Wire (Cured) C. 2 Hcls Glass (Cured)	29.0 Ksi	22.8	34.9
- 2	A. 7 Hoops Wire (Cured) B. - C. -	21.0 Ksi	15.8	27.5
- 3	A. 7 Hoops Wire (Gelled) B. 4 Hcls Wire (Cured) C. 2 Hcls Glass (Cured)	>18.0 Ksi	15.8	27.5
- 4	A. 2 Hcls Glass (Gelled) B. 7 Hoops Wire (Gelled) C. 2 Hcls Wire (Cured) D. 2 Hcls Glass (Cured)	12.0 Ksi	15.8	27.5
- 6	A. 2 Hcls Glass (Gelled) B. 9 Hoops Wire (Cured) C. 2 Hcls Wire D. 2 Hcls Glass (Cured)	17.5 Ksi	20.5	32.4
- 7	A. 2 Hcls Glass (Cured) B. 9 Hoops Wire (Gel) C. 4 Hcls Wire (Cured) D. 2 Hcls Glass (Cured)	19.0 Ksi	20.5	32.4
- 8	A. 2 Hcls Glass (Gel) B. 9 Hoops Wire (Cured) C. 2 Hcls Wire D. 4 Hcls Glass (Cured)	17.5 Ksi	20.5	32.4
- 9	Unwrapped	10.0 Ksi	0.0	9.3

\*Assumed liner burst strength of 0 Ksi

\*\*Assumed liner burst strength of 30 Ksi

In all but SN-2, the last layers were wound with 20 end E-glass roving. These layers allow easier handling of the steel/epoxy jacket and provide a machinable surface for future fittings in gun barrels. For the samples SN-4, 6, 7, and 8, one helical pattern (2 layers) of E-glass was helically wound as the initial layers. The rationale for this was to provide an interface between the ceramic liner and the wire wound jacket that would more uniformly distribute the point contact load of this initial wire layer. It was thought that excessive stress concentrations at these contacts would lead to premature failure in a pressure tested cylinder.

#### TESTING

An unwrapped Alumina liner was initially pressure tested to (a) check out testing equipment and sealing devices and (b) verification of the supplier's literature on the mechanical properties of the ceramic. This specimen and the wrapped specimens were pressure tested using a dead weight test machine. The specimens were pressurized using a pump-intensifier system. Pressure and strain gage output were recorded at selected pressure levels until the specimen burst. Sealing was accomplished with a series of rubber O-rings with leather and aluminum backup seals.

A hoop strain gage was mounted on the O.D. of the unwrapped liner so that the pressure vs strain could be monitored. A plot of this data is shown in Figure 8. The computed elastic modulus (E) from this data was  $54.5 \times 10^6$  versus the  $57 \times 10^6$  stated in the literature.

# ALUMINA CYLINDER

$$\sigma \Big|_{r=b} = 1.81 P = \left( \frac{2a^2}{b^2 - a^2} \right) P$$

WHERE  $a = 0.260''$ ,  $b = .377''$

## EXPERIMENTAL DATA

PRESSURE (KSI)	STRAIN ( $\mu\text{in/in}$ )
0	0
5	165
6	200
7	230
8	265
9	295
10	325

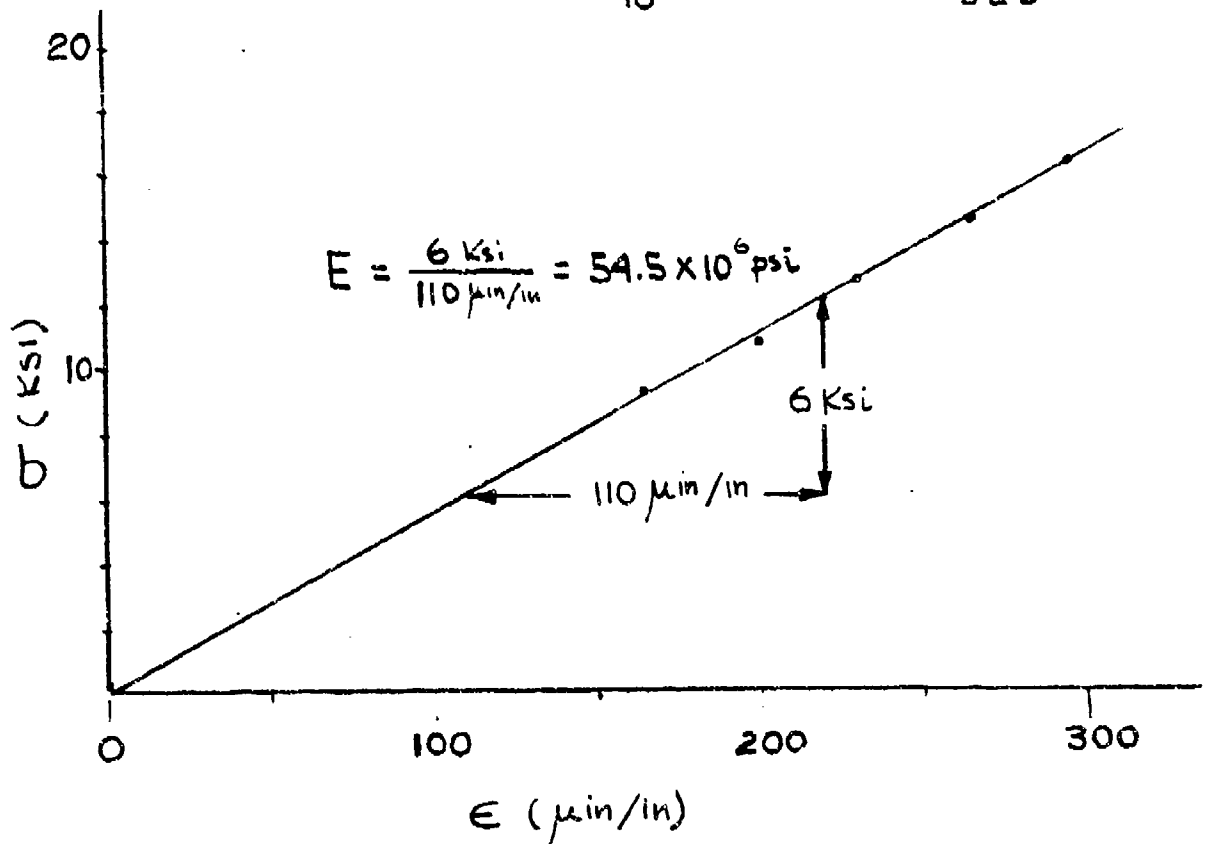


Figure 8. Pressure-strain data for typical 12.5 mm alumina liners

The seven composite jacketed cylinders were tested in the same manner as the unwrapped sample. Table 2 shows the burst pressure for each of the cylinders and the theoretical rupture pressure as computed by TENZAUTO.

NOTE: In the theoretical analysis of the cylinders, the hoop strength contribution of the helix layers (be they steel or glass) was not considered.

As mentioned previously, the cylinders SN-4, 6, 7, and 8 each contained an initial full helical pattern (2 layers) of fiberglass. These cylinders burst at pressures less than their predicted yield pressure. The other three cylinders without the initial layer of fiberglass burst at pressures within their predicted rupture pressures.

Initially, it was felt that the fiberglass layers would better distribute the point contact load from the wire and result in a stronger cylinder. In reality, the opposite occurred and weaker specimens were the result.

The best explanation for the lower results is that the initial helical fiberglass layers provided a low modulus interface ( $\sim 5 \times 10^6$  Psi) between the ceramic and the steel composite jacket. The low modulus interface allowed the liner to dilate more than desired before the higher modulus steel composite jacket provided the necessary restraint. This effect probably induced failure of the liner by prohibiting the jacket and liner from working as a unit in withstanding the internal pressure.

## II. 6.4 mm Tungsten-Carbon Alloy (CM-500) Liners

6.4 mm cylinders, fabricated by Chemetal Corporation, were provided for test and evaluation of material properties and strengths. The cylinders are fabricated using a chemical vapor deposition technique. The specific composition is proprietary, but the material is essentially a tungsten alloy.

This section will cover preliminary design, fabrication and testing of a CM-500 liner filament wound with high strength steel filaments embedded into an epoxy matrix. The CM-500 liner has an I.D. of 0.250 inches, an O.D. of 0.330 inches, and a length of 2.35 inches. In-house pressure tests have shown that liners of similar geometry have ruptured at pressures of 42 Ksi and 58 Ksi or at tensile stresses of 155 Ksi and 217 Ksi respectively.

Theoretical results, based on an assumed 155 Ksi tensile strength, show that an 86.9 Ksi max pressure capacity would be expected by filament winding the same liner with 5 hoop layers of 6 mil NS-355 wire with a 6 lb per end tension as shown in Table 3. Figures 9, 10, and 11 depict results obtained from TENZAUTO for such a construction, while Table 4 shows experimental results from the internal pressure test, the burst pressure was 80 Ksi (239 Ksi tangential stress) which shows close agreement with the computed value of 86.9 Ksi.

TABLE 3. DETAILS OF THE TUNGSTEN-CARBON CYLINDER

Liner-Chemetal's CM-500\*

- Tungsten-Carbon (CVD) Alloy
- I.D. = .250" O.D. = .330"
- Wall Thickness: = .040"
- Length: ~ 2.35"

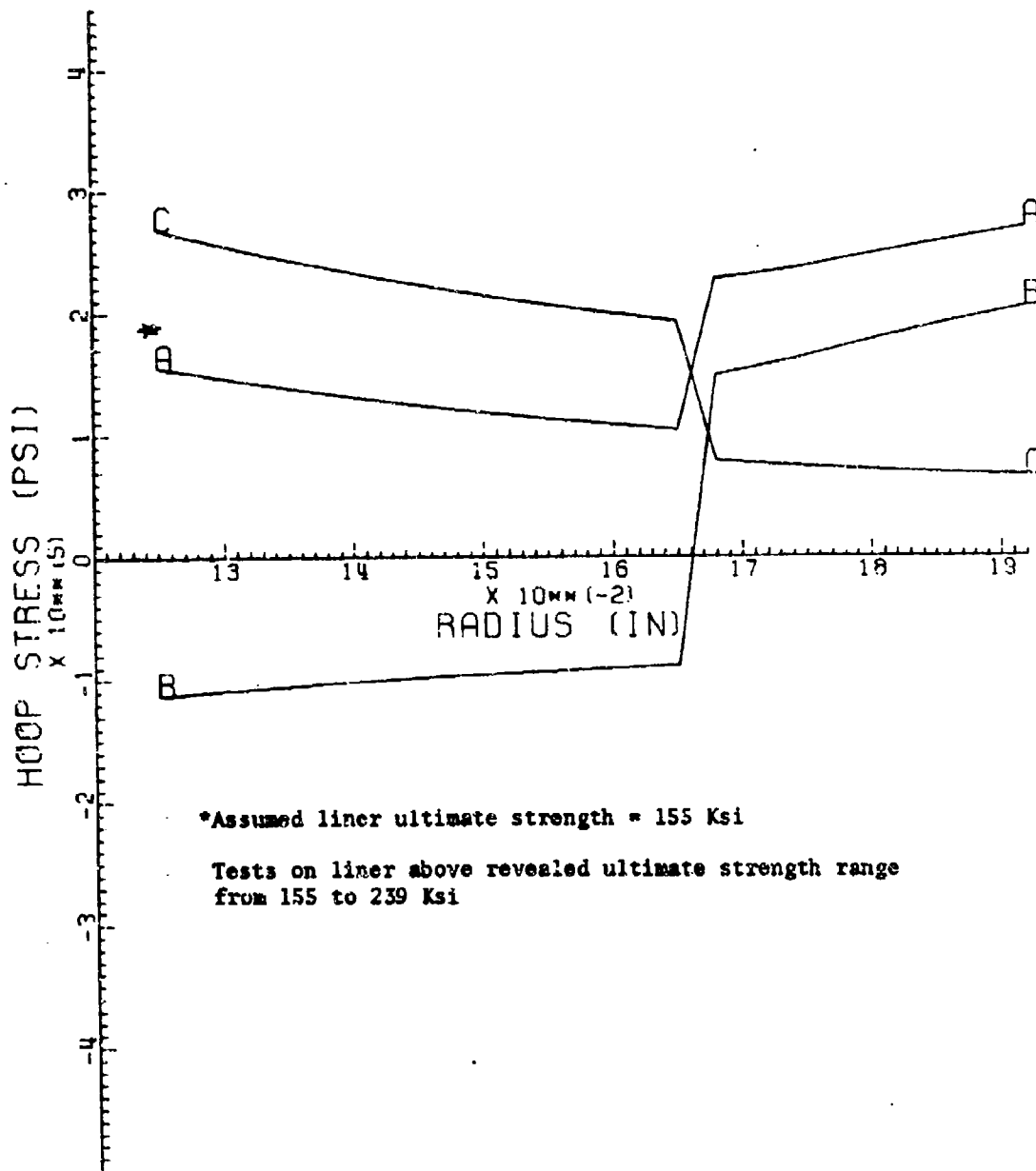
Winding:

5 Layers of 6 mil NS-355 wire/epoxy wound entire length. Dog bone shaped in order to assure rupture in the center section. Seven layers wound 0.5" from each end and nine layers wound 0.4" from each end.

Coverage = 164 ends/in/layer  
Tension = 6 lb/end

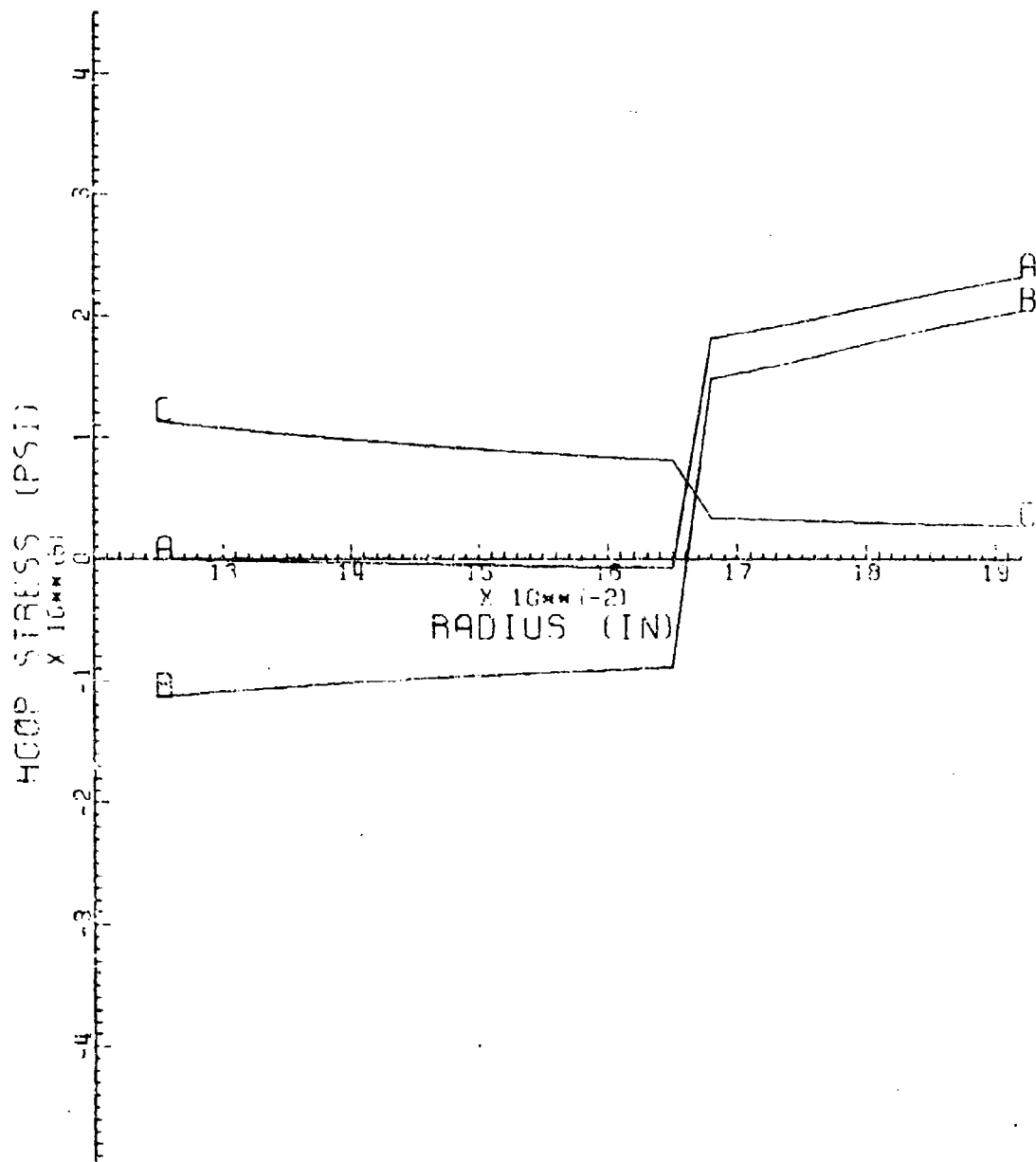
Overall length of cylinder was 2.35" and the ends were built up from 0.50" back then the resulting gage length is 1.35".

\*Chemetal  
Pacoima, CA



(PRESSURE = 86984 PSI)  
 SERVICE = A-A, RESIDUAL = B-B, ELASTIC = C-C

Figure 9. Stresses developed in 6.4 mm W-C alloy specimens (155 Ksi T.S.)



(PRESSURE= 36582 PSI)  
 SERVICE = A-A, RESIDUAL = B-B. ELASTIC = C-C

Figure 10. Stresses developed in 6.4 mm W-C alloy specimens (C Ksi T.S.)

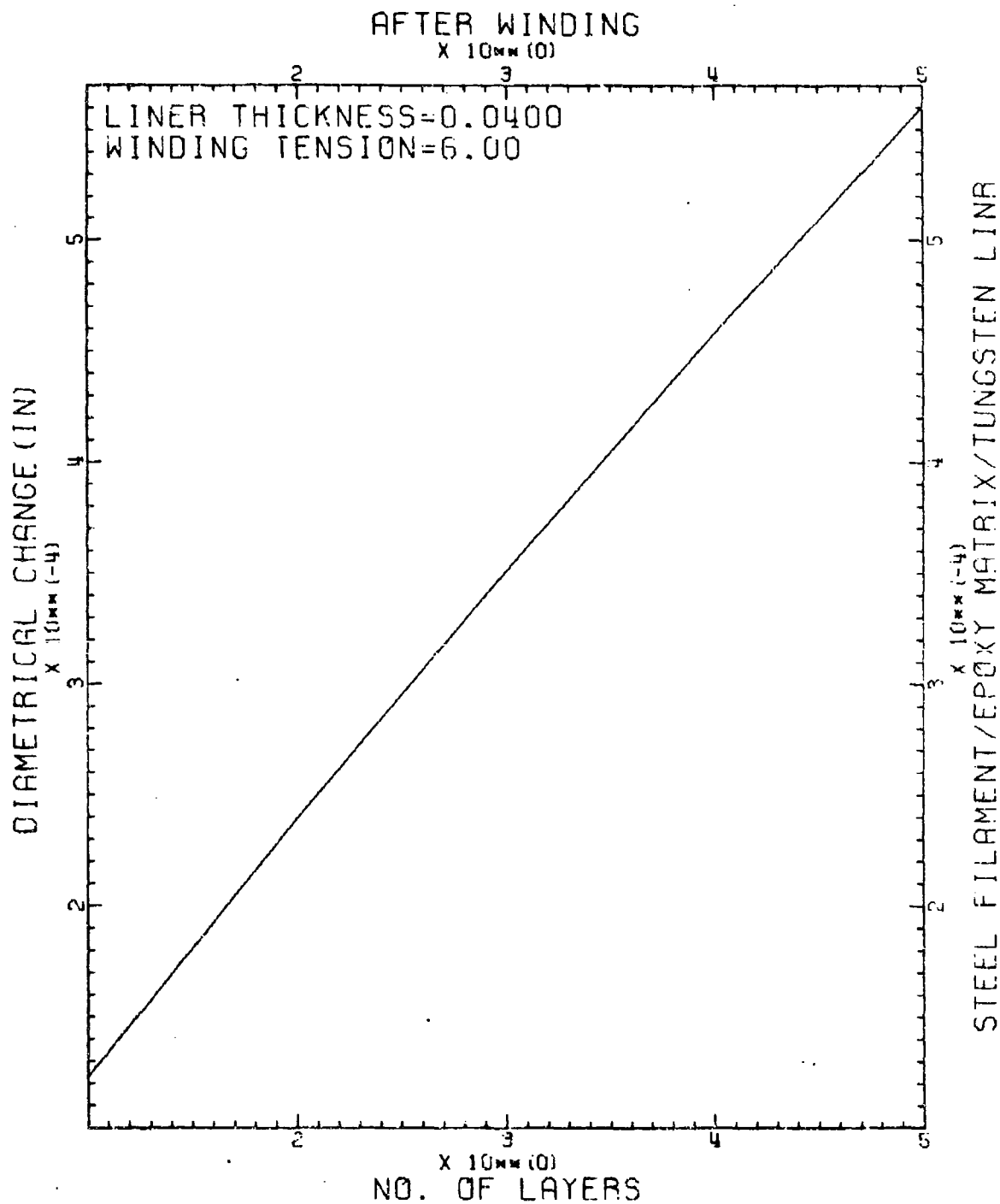


Figure 11. Diametrical change vs layers for 6.4 mm W-C specimens

TABLE 4. CALIBRATION OF THE 100 KSI LOAD CELL USED IN THE TESTING  
OF THE 6.4 MM (CM-500) COMPOSITE CYLINDERS

Pressure (Ksi)	Strain ( $\mu\text{in/in}$ )
0	010
10	161
20	309
30	459
40	609
50	759
60	912
70	1064
80	1216

Burst of filament wound specimen occurred at 1190  $\mu\text{in/in}$  or 80,000  
Psi pressure.

### III. 60 mm Ceramic Liners

The original goal was to fabricate a 10 inch long 60 mm I.D. composite cylinder capable of containing a design pressure of 70,000 psi. This concept required a 0.140" thick alumina liner with 65 hoop layers of winding. A series of events (or Phases) which lead to reassessment of the original goal is next presented.

#### PHASE I

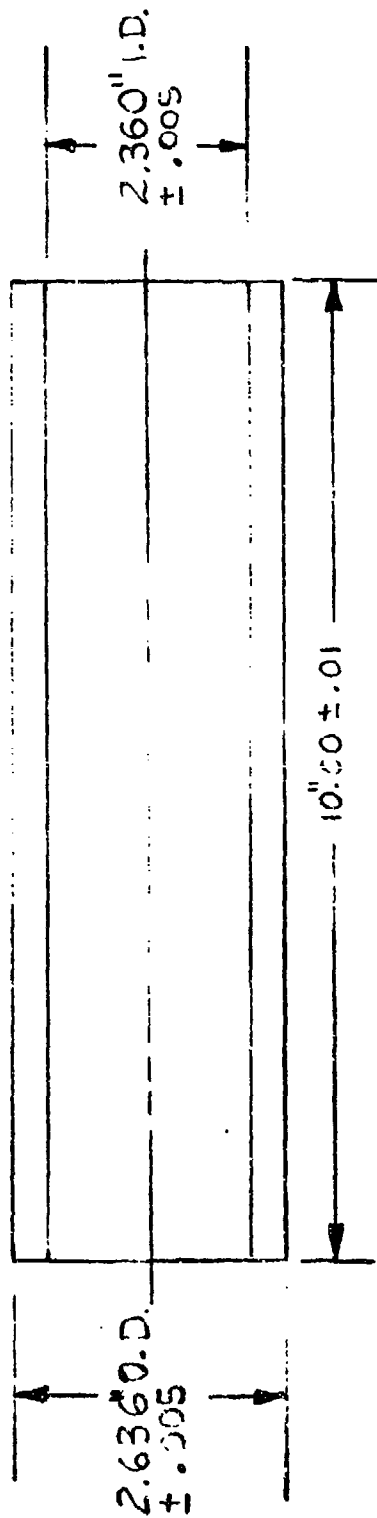
The series of samples involved in this phase use a 60 mm (2.360 in) I.D. Alumina liners with the steel wire composite jackets. A dimensional sketch of the liner is shown in Figure 12. The physical properties of the Alumina are the same as shown in Figure 4.

In order to experimentally determine the residual stresses during winding, two rosette type strain gages were internally mounted in the ceramic liners. These gages were aligned to record the liner's deflection, during winding, in the hoop, longitudinal and 45° direction.

All filament wound 60 mm samples used the same 6 mil NS-355 wire with epoxy/anhydride cured matrix as the composite jacket. The winding tension was fixed at 6 lb/end and the hoop coverage was maintained at 162 ends/in.

#### Specimen 60-1

This specimen was initially wound with 9 hoop layers, with no resin, to check out both the overall winding parameters and the continuity of the strain gages. Table 5 shows the strains recorded after the 3rd, 6th and 9th layers. This was done by stopping the winding and attaching the leads to a BLH Switch & Balancing Unit and the



CONCENTRICITY : T.I.R (TOTAL INDICATOR RUNOUT) = 0.005"

Figure 12. Sketch of 60 mm alumina specimens

induced strain on each of the six channels was recorded from a BLH Strain Gage Indicator. In addition, the specimen was held overnight in the winder with the winding tension maintained, to see if there would be any significant deflection change. The results in Table 5 indicate no significant change in deflection. After this "dry run", the wire was unwound and the cylinder was prepared for the actual winding operation. Table 5 also shows the strain data for the actual winding of specimen #60-1. The liner itself broke during the winding operation. About 1/3 of the way through layer #20, the specimen separated about 1 inch from the end. It was a definite failure due to longitudinal loads because as shown in Figure 13 the fracture was a transverse separation of the liner at this location.

A closer look at the data in Table 5 and the mechanical properties of Alumina can explain the failure of the specimen. After layer #18, the average longitudinal strain recorded from gages #6L and #9L was +483  $\mu\text{in/in}$ . In addition, the computed elastic modulus (E) for this alumina material was  $55 \times 10^6$  Psi while the tensile strength ( $\sigma$ ) is 30,000 Psi.

If  $\epsilon = \sigma/E$  then  $\epsilon_{\text{max}} = \frac{30,000}{55 \times 10^6} = \sim 550 \mu\text{in/in}$ . This indicates that the max tensile strain that Alumina can take is  $\sim 550 \mu\text{in}$ , and after layer #18 a strain of +485  $\mu\text{in/in}$  already was generated. Therefore the additional longitudinal strain caused by layers #19 and #20 must have exceeded the upper strain limit of the ceramic and caused its transverse failure.

TABLE 5. INTERNAL STRAIN DATA OF SPECIMEN 60-1

DRY RUN

Channel Gage Type	<u>GAGE #1</u>			<u>GAGE #2</u>		
	4 $\epsilon_H$	5 $\epsilon_{45^\circ}$	6 $\epsilon_L$	7 $\epsilon_H$	8 $\epsilon_{45^\circ}$	9 $\epsilon_L$
Start	0	0	0	0		0
1 + 3	- 335	-110	+180	-335		+170
4 + 6	- 725	-250	+270	-670	No Readings	+240
7 + 9	-1090	-410	+360	-1035		+310
Held Overnight	-1080	-410	+360	-1025		+310
			<u>#60-1</u>			
Start	0	0	0	0	-	0
1 + 3	- 375	-160	+ 80	- 365		+ 75
4 + 6	- 735	-330	+145	- 720		+160
7 + 9	-1080	-470	+225	-1045		+235
10 + 12	-1410	-590	+300	-1375		+325
13 + 15	-1720	-745	+410	-1695		+395
16 + 18	-2010	-860	+490	-1980		+475

It now becomes apparent that although Alumina's high compressive strength allows for exceedingly high compressive hoop loads, some way must be found to prevent its axial displacement or premature failure will result.

It is also important to note that during firing, the moving pressure front introduces bending stresses that result in longitudinal tensile stresses. Thus it is not sufficient to insure that the longitudinal tensional strain induced during fabrication is less than the critical value. It must be sufficiently below to permit a sufficient margin to accommodate the longitudinal firing stress.

#### Specimen 60-2

Two possible solutions to limiting the elongation of the liner were attempted with this specimen. The first called for excessive tightening of the retaining nuts periodically throughout the winding, and the second was to provide helical windings in the specimen in an attempt to hold back the elongation.

Both solutions required slight changes in the fixturing which would allow for (a) excessive wrench tightening of the nuts, and (b) the use of an aluminum ring which would be helically wound into the specimen.

Table 6 is a summary of the strain data recorded during the winding and gelling of specimen 60-2. Actual readings were taken every third hoop layer.

The primary aim during the winding of this specimen was to limit the longitudinal strain to  $< 500 \mu\text{in}/\text{in}$ . This was initially done by tightening the retaining nuts to a torque which would induce a slight negative strain (compressive before winding). During the winding

TABLE 6. INTERNAL STRAIN DATA OF SPECIMEN 60-2

Channel Gage Type	GAGE #1			GAGE #2		
	11 eH	12 e45°	13 eL	14 eH	15 e45°	16 eL
Start	0	0	0	0	0	0
Tighten Nuts	0	0	- 35	0	0	- 40
1 - 12 Hoops	-1245	- 585	+195	-1205	- 640	+165
13 - 21 Hoops	-2075	- 945	+415	-2065	-1010	+355
After Gel	-2030	- 950	+235	-2055	-1080	+160
1 & 2 Helical	-2155	-1025	+155	-2195	-1160	+150
After Gel	-2160	-1055	+105	-2225	-1205	+ 95
22 - 33 Hoops	-3070	-1425	+360	-3115	-	+350
After Gel	-3040	-1465	+330	-	-	+320
3 & 4 Helical	-3140	-1520	+325	-	-	+320
After Gel	-3130	-1520	+325	-	-	+305
Retighten Nuts	-3080	-1550	+225	-	-	+210
34 - 45 Hoops	-3830	-1910	+450	-	-	+360
After Gel	-3785	-1830	+435	-	-	+335
5 & 6 Helical	-3875	-1875	+465	-	-	+330
Glass Helical	-	-	-	-	-	-
After Gel	-3900	-1910	+410	-	-	+300
Release Nuts	-3645	-1445	+925	-	-	+860

operation, these nuts were also retightened before the 4th, 7th, and 10th hoop layers and again before the 34th hoop layer.

This continual tightening of the nuts, along with the application of 6 helical patterns (12 layers) aided in keeping the strain  $< 500$   $\mu\text{in/in}$ . The first gel cycle, after the initial 21 hoops, reduced the longitudinal strain by  $\sim 190$   $\mu\text{in/in}$  while the second gel cycle, after the initial 2 helical patterns, reduced longitudinal strain by  $\sim 50$   $\mu\text{in/in}$ .

The combination of continual tightening of the nuts; the utilization of 6 helical patterns; and the 6 "gel" cycles enables the winding of 45 hoop layers and still maintained the longitudinal strain to  $< 500$   $\mu\text{in/in}$ . A final fiberglass helical layer was introduced for ease of handling.

After the final "gel" cycle, the retaining nuts were slowly released and the strain was monitored. As soon as the torque was released, a "crack" was heard within the specimen. Inspection of the sample, after removal from the fixture, showed a  $360^\circ$  transverse fracture at a location of  $3 \frac{1}{2}$  inches from one end of the liner.

Figures 13 through 19 summarize the results on this phase of the 60 mm ceramic liner study from which it can be concluded that other techniques must be utilized to reduce the longitudinal tensile stresses induced during fabrication.

Figure 13 shows (a) a ceramic liner, (b) the first filament wound cylinder (60-1) which resulted in tensile failure after 19 hoop layers, and (c) the second filament wound cylinder (60-2) comprising 45 hoop layers and 6 helical layers (12 thicknesses). The composite jacket

consisted of a six-mil steel filament embedded in an epoxy matrix. Note the lead wires from the 45° rosettes.

Figure 14 shows correlation between experimental results and theoretical output of computer program TENZAUTO. These results pertain to the first filament wound cylinder (60-1).

Figure 15 shows correlation between theory and experiment for 60-2.

Figures 16 and 17 show the theoretical residual stresses (curve B-B) as introduced by the filament winding process for 45 layers wound with 6 lb/end tension. The service stress (curve A-A) of Figure 16 produced by an internal pressure of 48,902 Psi considers a 30,000 Psi tensile strength for the ceramic. Figure 17 considers the ceramic liner to have zero tensile strength hence a reduction in the theoretical component, and prevents, hopefully, micro-cracks from forming since the ceramic is not under tension during the service cycle.

Figure 18 shows hoop strain gage data as a function of the layers. The hoop strain when translated into displacement data correlates within 10% of the theoretical data, see Figure 15. Also note that after 45 hoop layers and the 6 helical layers the recorded hoop strain of 3830  $\mu\text{in/in}$  when multiplied by the modulus of Elasticity of Alumina ( $55 \times 10^6$  Psi) gives a residual hoop stress of approximately 200 Ksi which is 10% less than the predicted one.

Figure 19 shows the longitudinal strain as a function of (1) hoop and helical layers, (2) load induced by mandrel fixture, and (3) temperature developed during the gelling process.

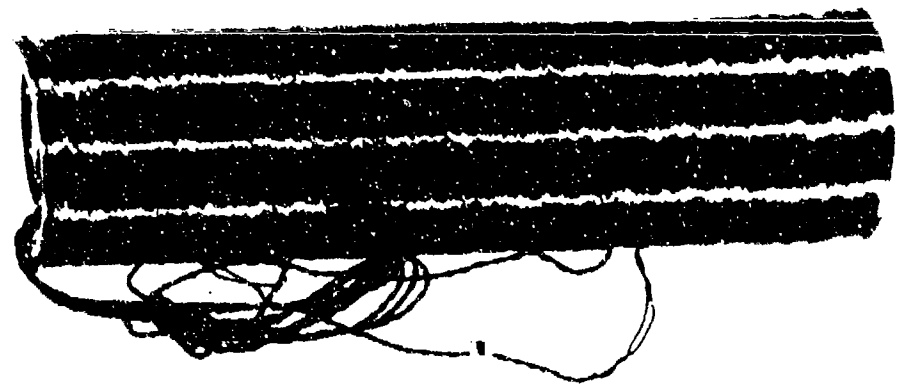
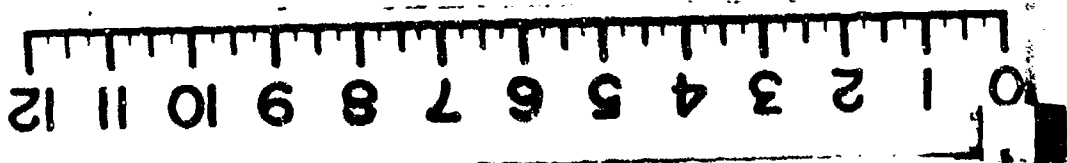


Figure 13. View of 60 mm specimens from Phase I

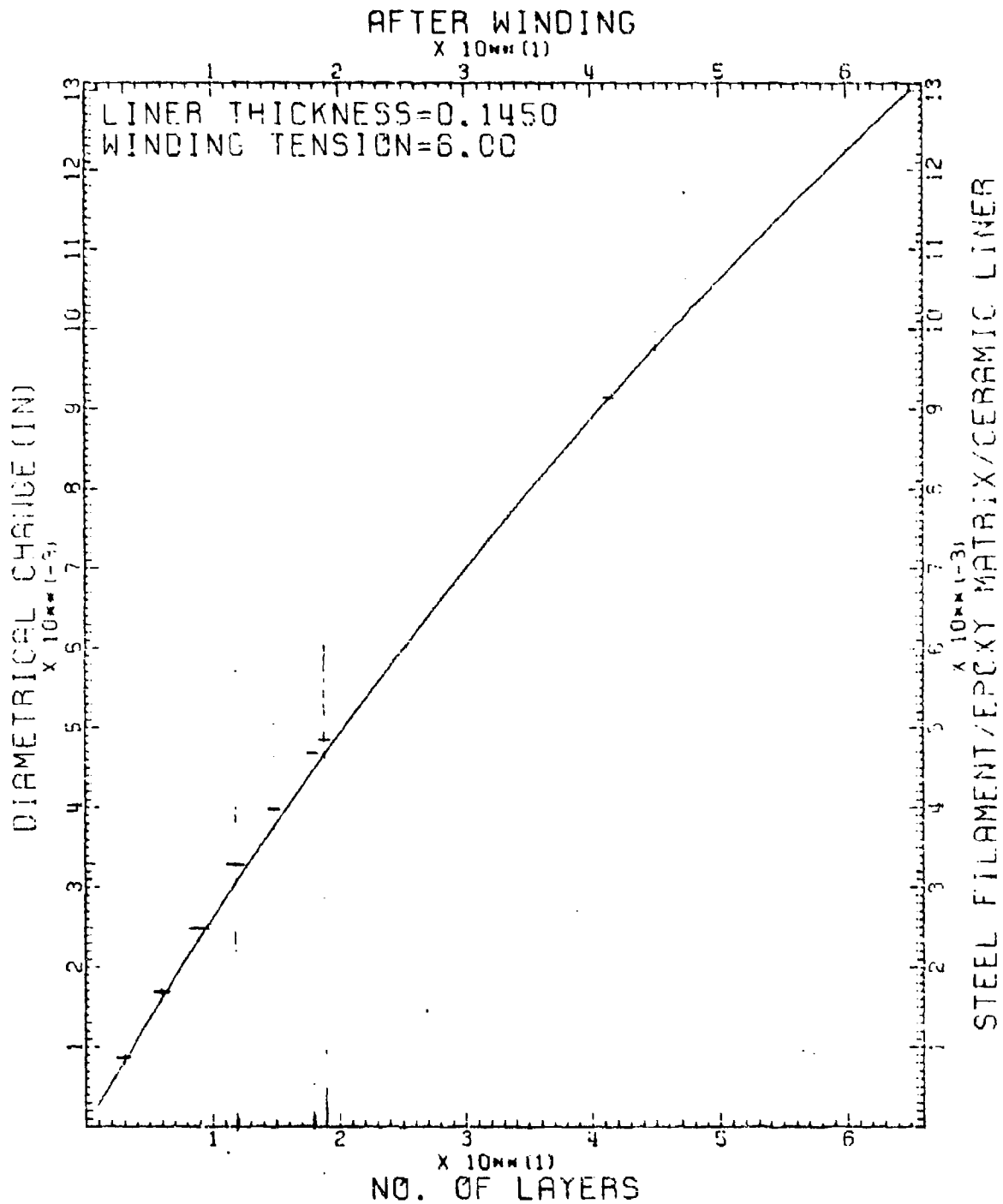


Figure 14. Diametrical change vs layers for specimen 60-1

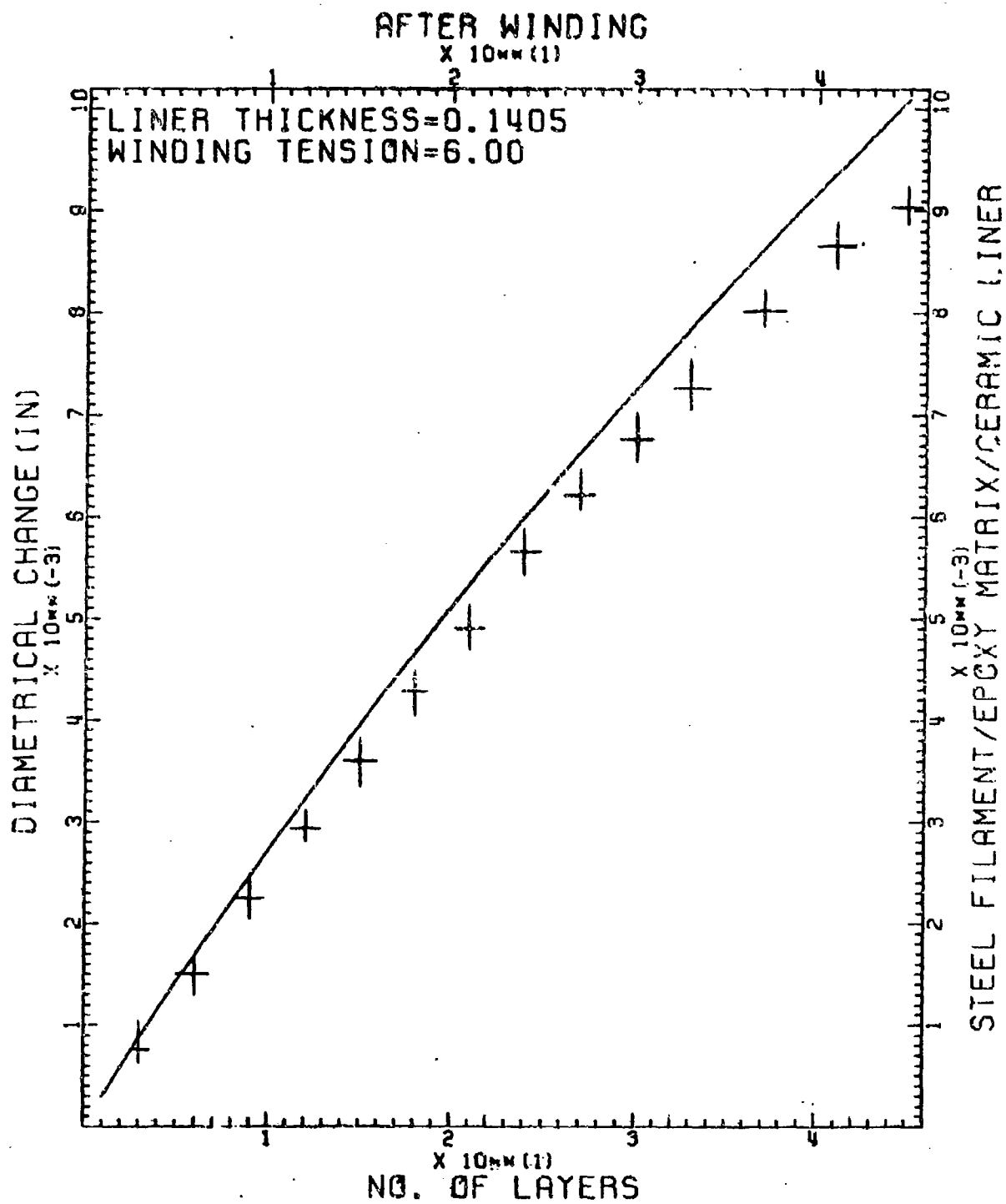
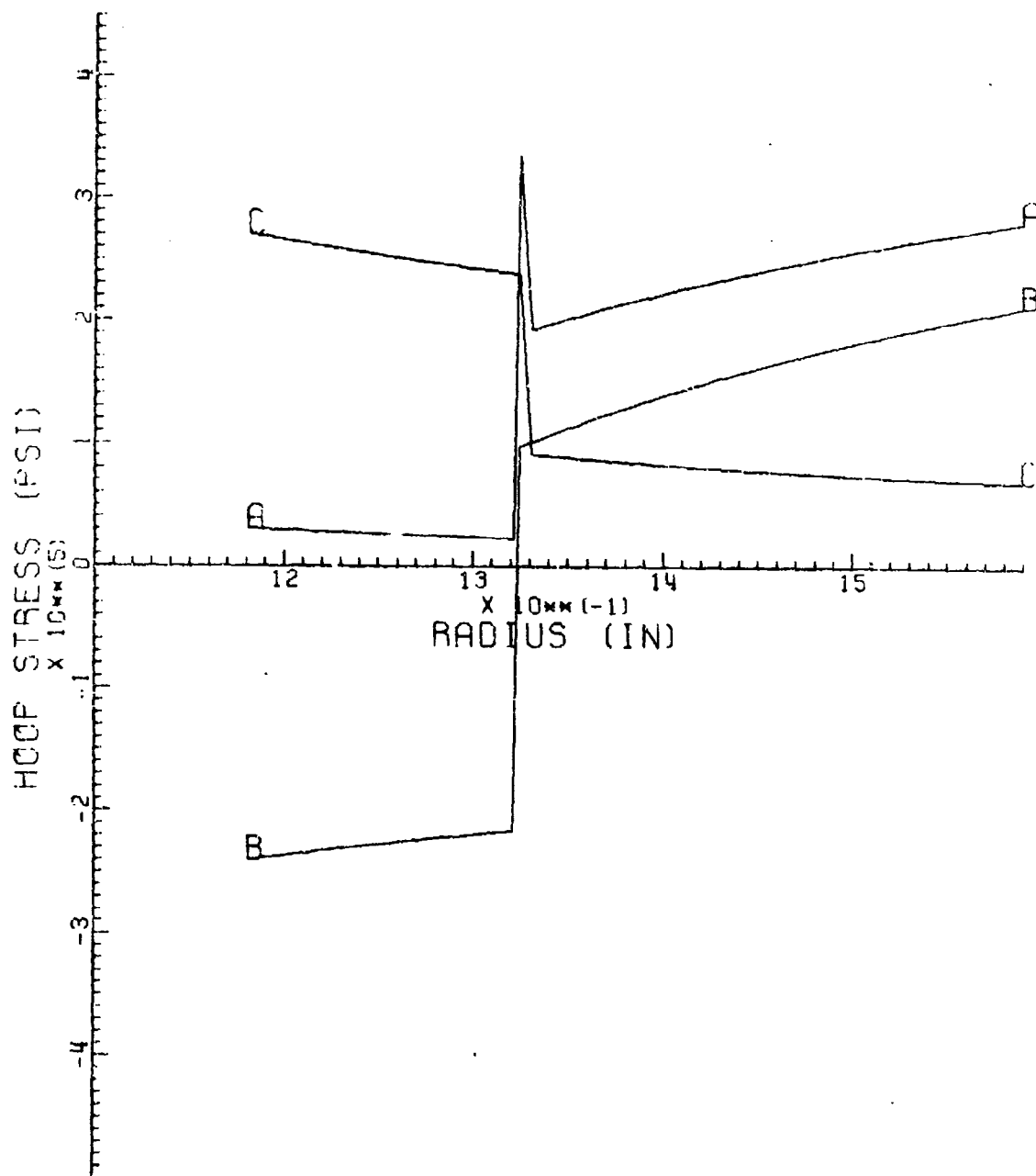
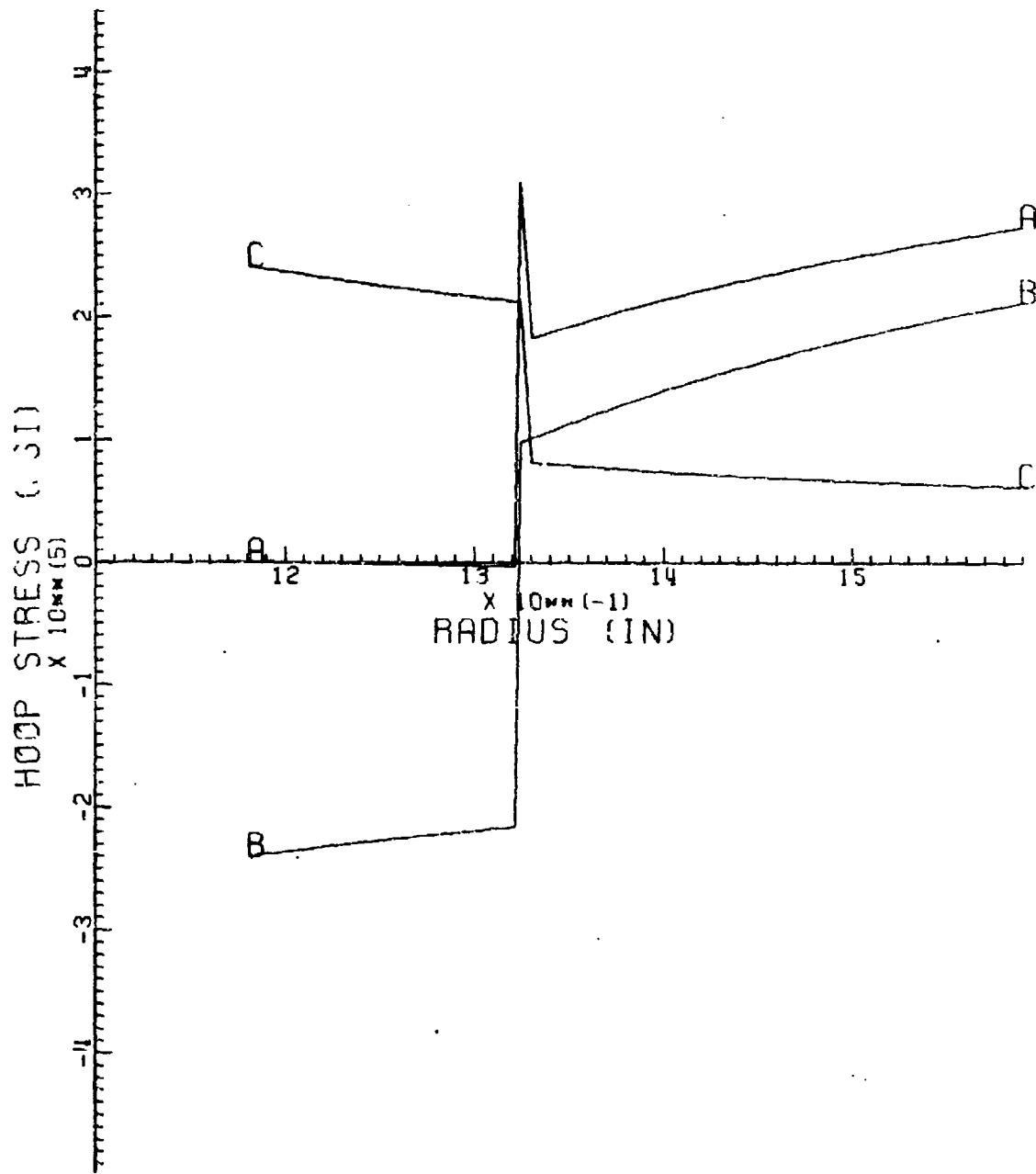


Figure 15. Diametrical change vs layers for specimen 60-2



(PRESSURE = 48902 PSI)  
 SERVICE = A-A, RESIDUAL = B-B, ELASTIC = C-C

Figure 16. Stresses developed in specimen 60-2 with a 30 Ksi T.S.



(PRESSURE = 43472 PSI)  
 SERVICE = A-A, RESIDUAL = B-B, ELASTIC = C-C

Figure 17. Stresses developed in specimen 60-2 with a 0 Ksi T.S.

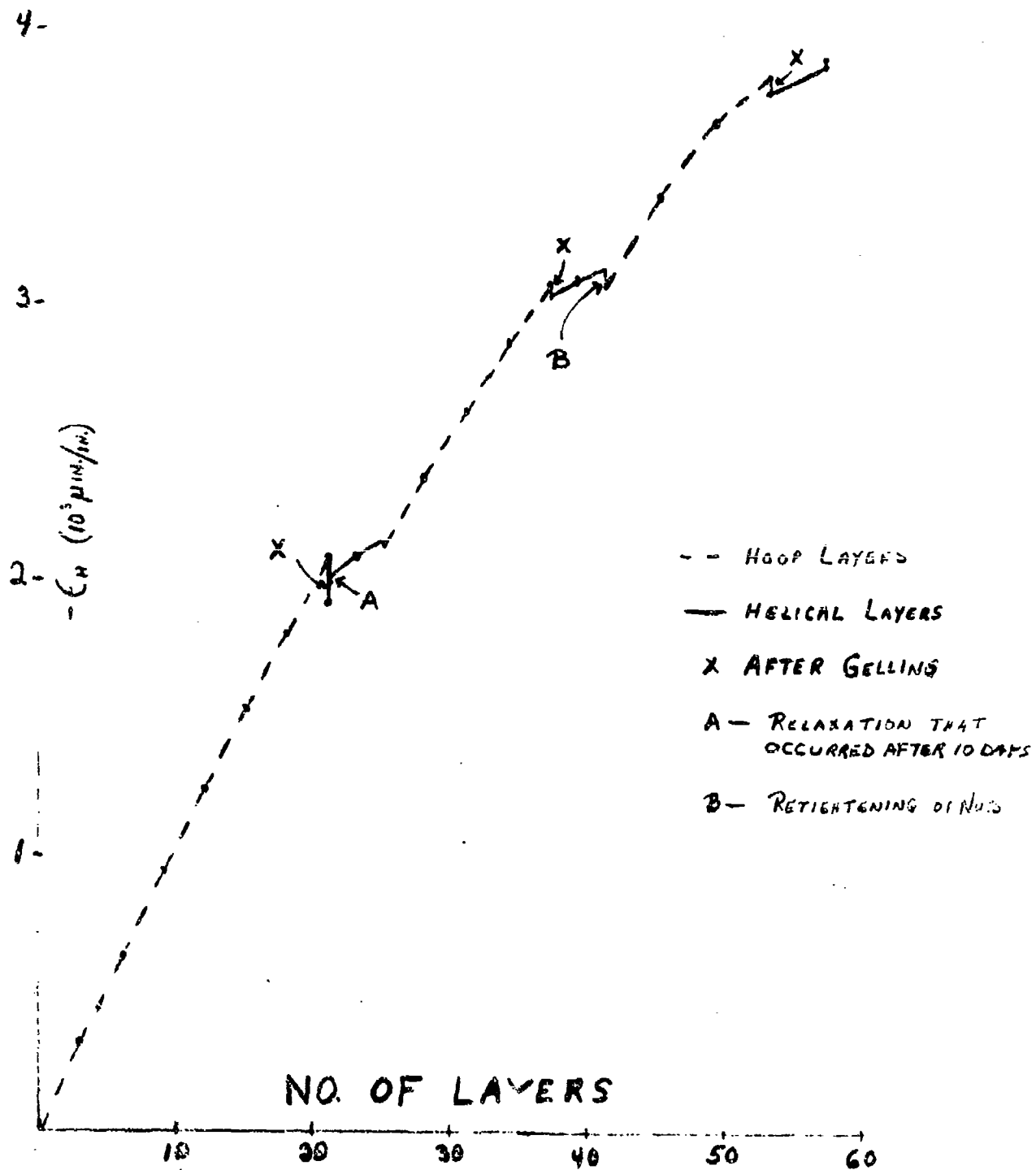


Figure 18. Hoop strain vs wound layers of specimen 60-2

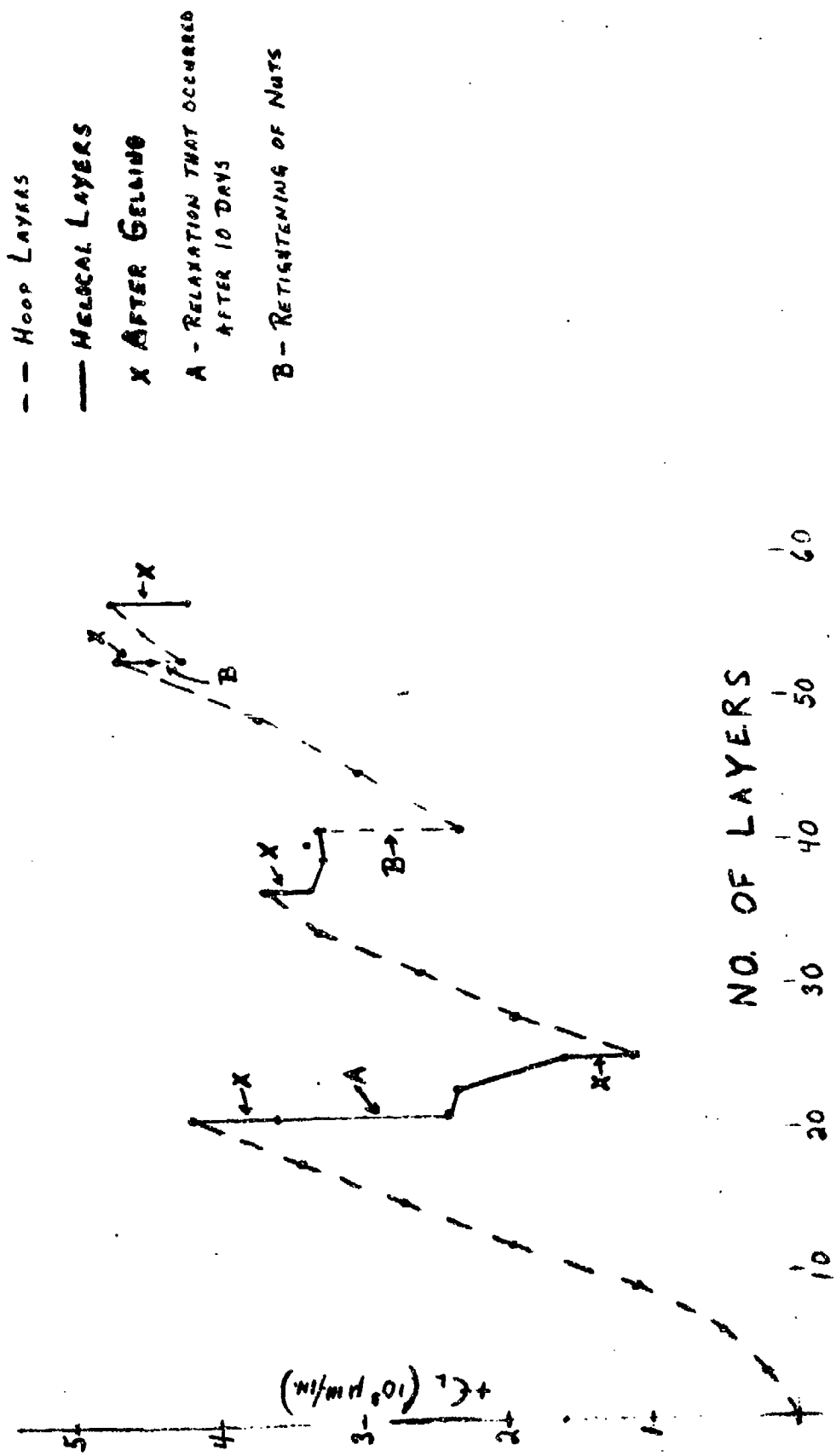


Figure 19. Longitudinal strain vs wound layers of specimen 60-2

## PHASE II

From Phase I it was concluded that other techniques were required to prevent failure of the ceramic liner.

### Specimen 60-3

This specimen was prepared in another attempt to induce a high compressive longitudinal load on the ends of the liner. Table 7 shows the corresponding strain data with the fabrication steps.

The retaining nuts were initially tightened with wrenches to induce  $\sim -130 \mu\text{in/in}$  compressive strain. After the gel cycle of the first 20 hoop layers the specimen was again compressively torqued on a Universal Torque Machine.

The specimen was slowly torqued to a final load of 10,000 in-lb. Table 8 shows the longitudinal strain data that was continually monitored on channel #1 as the torque was applied.

Table 8 indicates that the 10,000 in-lb torque induced a total compressive longitudinal strain on the liner of  $-545 \mu\text{in/in}$ .

The specimen was returned to the winding machine and 20 additional hoop layers were applied. In this case, the following gel cycle resulted in an increased longitudinal strain. The sample was then cured for 2 hours at  $350^\circ\text{F}$  to determine what effects the high temperature cure would have on the strain.

The data from Table 8 indicates only a small increase in longitudinal strain because of the cure cycle. For this reason, the decision was made to wind to the desired 65 hoop layers.

TABLE 7. INTERNAL STRAIN DATA OF SPECIMEN 60-3

Channel Gage Type	GAGE #1			GAGE #2		
	3 eH	2 e45°	1 eL	6 eH	5 e45°	4 eL
Start	0	0	0	0	0	0
Tighten Nuts	+ 25	- 75	-150	+ 50	- 20	-110
1 - 5 Hoops	- 665	- 365	-150	- 620	- 350	-120
6 - 10 Hoops	-1080	- 420	+ 15	-1020	- 450	+ 50
11 - 15 Hoops	-1575	- 570	+ 90	-1160	- 500	+260
16 - 20 Hoops	-1975	- 660	+235	-1420	- 560	+420
After Gel	-1520	- 610	+160	-1040	- 490	+210
Torque Mach. 10,000 in-lb (Compression)	-1445	- 910	-385	- 775	- 720	-375
21 - 25 Hoops	-1790	-1055	-345	-1440	- 930	-235
26 - 30 Hoops	-2325	-1170	-240	-1930	-1085	-160
31 - 35 Hoops	-2715	-1260	-130	-2015	-1140	+ 25
36 - 40 Hoops	-3080	-1360	- 30	-2370	-1260	+110
After Gel	-2590	-1170	+ 30	-1760	- 970	+200
After Cure	-2600	-1125	+125	-1675	- 885	+240
41 - 45 Hoops	-2970	-1225	+230	-2030	-1025	+310
46 - 50 Hoops	-3130	-1310	+340	-2380	-1150	+385
51 - 55 Hoops	-3670	-1370	+450	-2590	-1250	+460
56 - 60 Hoops	-4000	-1435	+520	-2910	-1365	+550
61 - 65 Hoops	-4290	-1490	+680	-3180	-1450	+625
After Gel	-3850	-1440	+520	-2565	-1305	+410
100 in-lb			+485			+345
160 in-lb			+480			+290
200 in-lb			+470			+265
260 in-lb			+430			+230
300 in-lb			+425			+200
Release Torque on Retaining Nuts	-3735	-1220	+955	-2625	-1260	+660
Recheck before testing (1 week later)	-3705	-1255	+955	-2640	-1310	+625

TABLE 8. LONGITUDINAL STRAIN VS TORQUE APPLIED TO SPECIMEN 60-3

<u>Torque (in-lb)</u>	<u>Strain (<math>\mu</math>in/in)</u>	<u>Torque (in-lb)</u>	<u>Strain (<math>\mu</math>in/in)</u>
0	+160	6500	-310
2500	+ 80	7000	-345
3000	+ 20	7500	-
3500	- 35	8000	-380
4000	-105	8500	-400
4500	-150	9000	-415
5000	-200	9500	-
5500	-	10000	-425
6000	-285	<u>Dump Load</u>	-385

After the gel cycle, the longitudinal strain gage indicated the resultant strain was +520  $\mu\text{in/in}$ . Theoretically this places the liner at its elastic limit. It was felt that if the retaining nuts were loosened, the liner would elongate further and crack. Therefore, two retaining collars with the assistance of 4 each 3/8" threaded rods (as shown in Figure 20) were applied to prevent further axial elongation. The nuts on the four rods were torqued to 300 in-lb. Table 7 also shows the recorded compressive strain from the longitudinal gages at various recorded torque levels.

The specimen and fixturing were returned to the Torque Machine and the large retaining nuts were slowly loosened. Upon removal, the longitudinal strain increased another 500  $\mu\text{in}$ , to a cumulative total of over 1000  $\mu\text{in}$ . This strain is almost double the elastic strain limit of the ceramic.

The ceramic was immediately checked for cracks but none were apparent even with the liquid dye penetrant technique. A week later utilizing the same liquid dye penetrant, indications of circumferential cracks was apparent.

Figures 21, 22 and 23 summarize the theoretical results of Phase II, assuming a filament winding of 65 hoop layers. The service stress, (A-A) of Figure 21, produced by an internal pressure of 70.5 Ksi considers a tensile strength of 30 Ksi for the ceramic. Figure 22 considers zero tensile strength and, therefore, a reduction in the theoretical pressure capacity (64.5 Ksi).

Figure 23 plots diametrical change vs number of layers. The dotted curve is a plot of the experimental curve if we neglect the intermittent stages (A-D) which decrease strain. This curve agrees nicely with the theory.

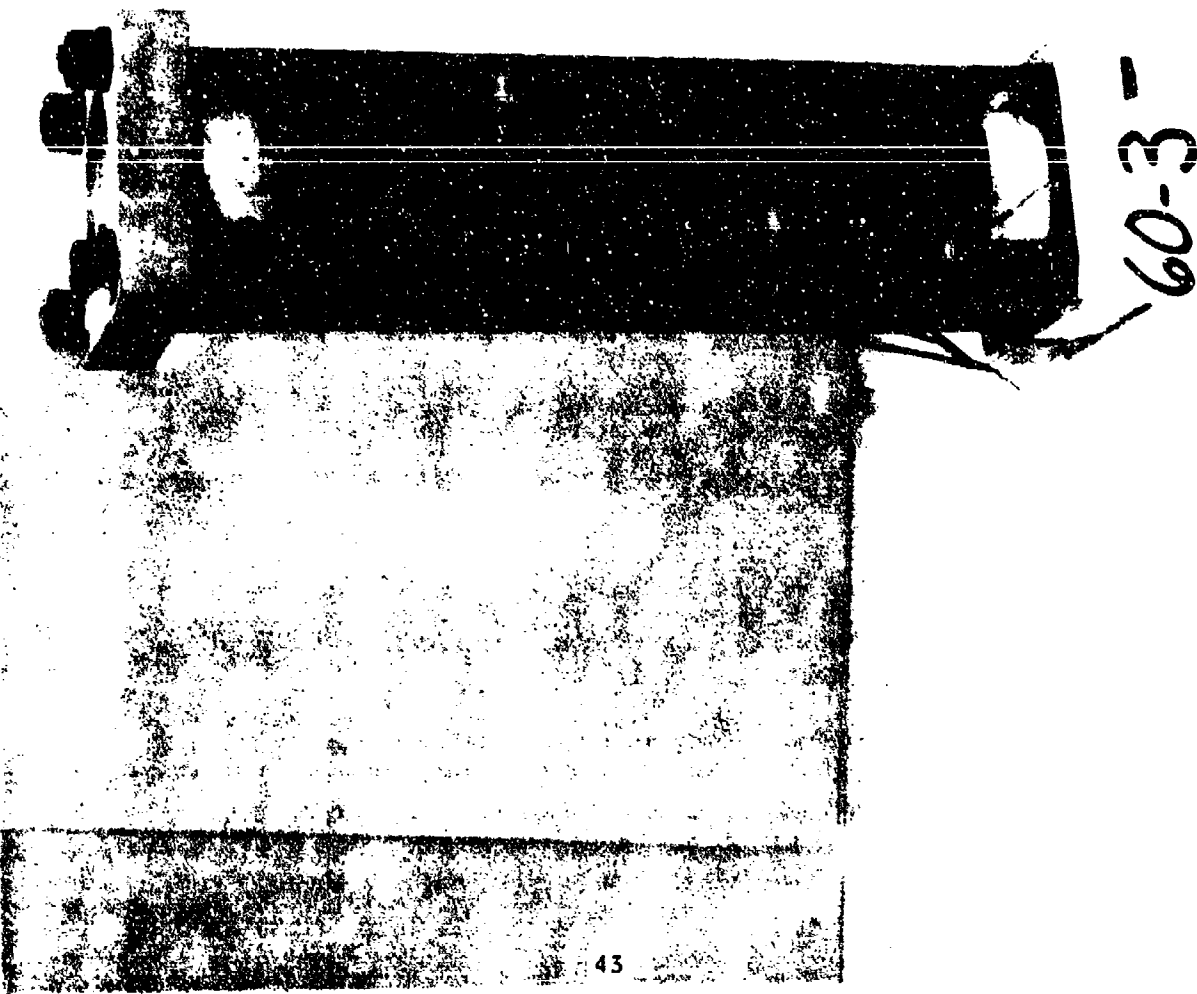
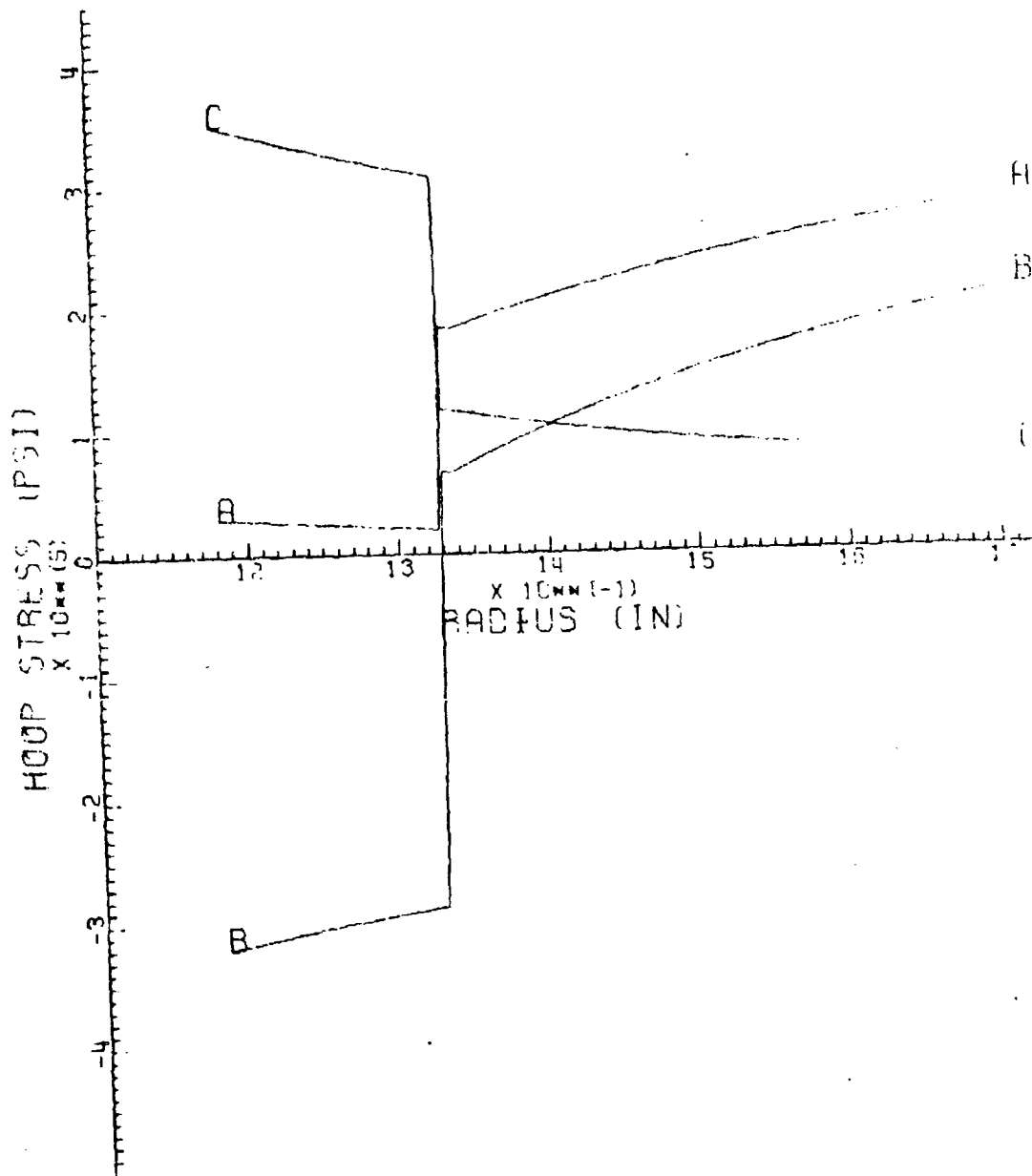
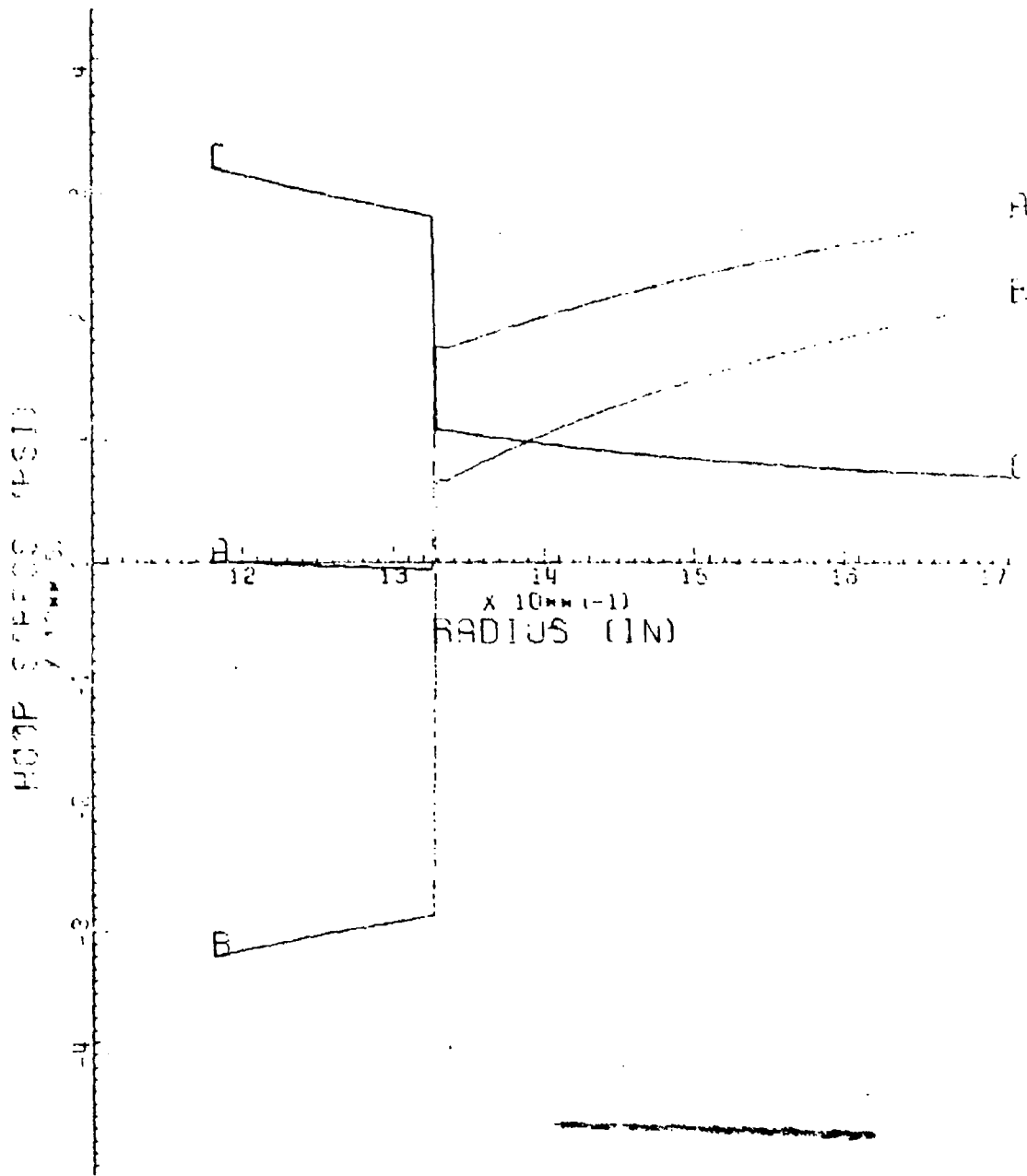


Figure 20. View of finished specimen 60-3 used in Phase I!



(PRESSURE = 70505 PSI)  
 SERVICE = A-A, RESIDUAL = B-B, ELASTIC = C-C

Figure 21. Stresses developed in specimen 60-3 with a 30 Ksi T.S.



(PRESSURE = 64466 PSI)  
 SERVICE = A-A, RESIDUAL = B-B. ELASTIC = C-C

Figure 22. Stresses developed in specimen 60-3 with a 0 Ksi T.S.

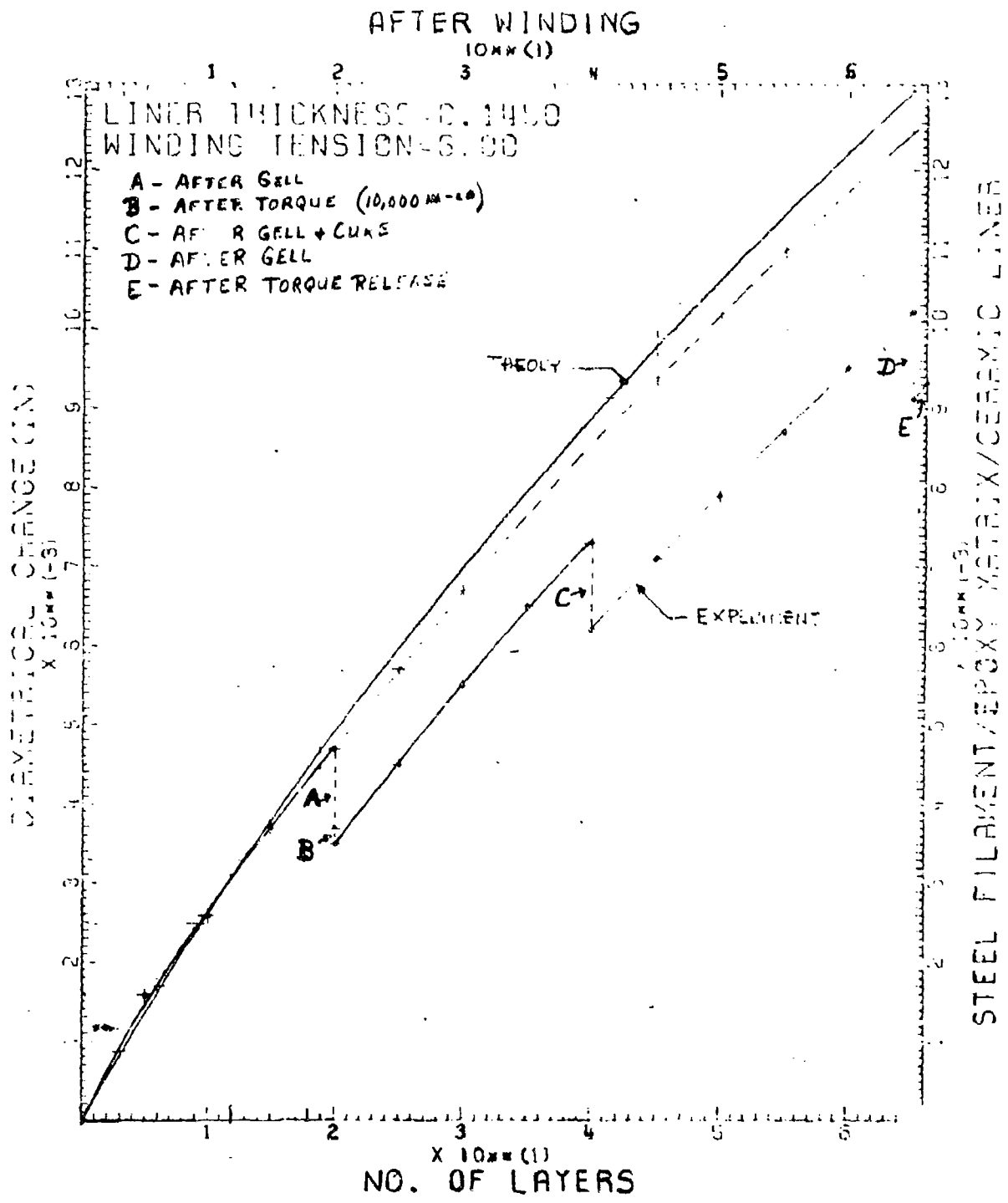


Figure 23. Diametrical change vs wound layers of specimen 60-3

### PHASE III

Since the mechanical locking arrangement did not seem feasible for inducing compressive longitudinal stresses a new concept was introduced. This called for the application of a shrunk-fit metallic sleeve between the liner and composite jacket. The first attempt used a 0.190" wall aluminum sleeve machined for a 0.002" radial interference fit at R.T. (Room Temperature). This 0.002" interference should have provided a -35,000 Psi longitudinal stress or a compressive strain reading of -700  $\mu\text{in}/\text{in}$ . If successful, this sleeve would have allowed the winding of 65 layers without relying on mechanical means for restraining the ends.

The formula which predicts the axial holding force of a shrunk fit cylinder relies on an accurate value of the coefficient of friction. Initial computations assumed a value of 0.3.

An aluminum alloy (6061) was machined to provide a 0.190" wall and an internal radius of 1.3160". This radius would provide the desired .002" radial interference when shrunk-fit on the 1.3181 outside radius of the Alumina liner.

The aluminum jacket's inside radius expands at a rate of 0.0017"/100°F and therefore a  $\Delta T$  of ~ 125°F is all that is necessary for a size for size fit. The machining tolerances of both cylinders over the 10 in. length require a much larger  $\Delta T$  to provide for easy insertion of liner into jacket. The shrink fitting was done at an oven temperature of 475°F (400  $\Delta T$ ) and no problems were experienced during the shrinking process on this specimen (60-5).

The ceramic liner was gaged internally with 2 each rosette type strain gages ( $0^\circ$ ,  $45^\circ$ ,  $90^\circ$ ). The data from the longitudinal gages shown in Table 9 indicated a compressive strain of  $-270 \mu\text{in/in}$  which corresponds to an induced stress of  $-15,000 \text{ Psi}$ . This stress is less than  $1/2$  of that expected. Reasons for this drop could be due to erroneous gage readings and/or an incorrectly assumed friction coefficient.

A second test cylinder (60-6) of Aluminum jacket/ceramic liner was prepared in the exact manner as the above. The shrink-fit strain data (Table 9) appears to vindicate the gages and pinpoint our lower longitudinal stress values on the friction coefficient.

This second cylinder was hoop wound with 20 layers of the 6 mil NS 355 wire. The winding tension was 6 lb/end with an average coverage of 162 ends/in/layer. Table 10 shows the resultant strain data recorded during the winding operation.

This cylinder, although indicating that the longitudinal strain was within the elastic limit of the ceramic, developed circumferential cracks approximately 30 minutes after the retaining nuts were removed. These cracks appeared at both ends ~ 1 to 2 inches from each end.

The data shown in Table 10 are the strains induced only by the winding. If the worst longitudinal strain (gage #4) is analyzed, one finds a tensile strain of  $+450 \mu\text{in/in}$ . This is near the alumina's elastic strain limit. However, the induced residual longitudinal stress that was recorded from the shrink-fit process was  $-255 \mu\text{in/in}$ . Adding the two values will result in a net tensile strain of  $+195 \mu\text{in/in}$  which is well within the elastic limit of the ceramic. Yet a few minutes

TABLE 9. SHRINK-FITTING STRAINS INDUCED IN 60 MM ALUMINA SPECIMENS

SN	GAGE #1			GAGE #2		
	#1 <sub>L</sub>	#2 <sub>45°</sub>	#3 <sub>H</sub>	#4 <sub>L</sub>	#5 <sub>45°</sub>	#6 <sub>H</sub>
60-5						
After Cool	-280	-270	-220	-260	-300	-250
24 Hrs Later	-290	-290	-240	-280	-320	-270
60-6						
After Cool	-215	-250	-250	-250	-250	-270
24 Hrs Later	-220	-250	-250	-260	-240	-275

TABLE 10. INTERNAL STRAIN DATA DURING FABRICATION OF SPECIMEN 60-6

No. of Layers	GAGE #1			GAGE #2		
	#1 <sub>L</sub>	#2 <sub>45°</sub>	#3 <sub>H</sub>	#4 <sub>L</sub>	#5 <sub>45°</sub>	#6 <sub>L</sub>
0	0	0	0	0	0	0
Tighten Nuts	-430	-280	- 40	-420	-275	- 40
1 5	-350	-430	- 500	-310	-395	- 500
6 10	-240	-555	- 930	-190	-515	- 830
11 20	-115	-770	-1575	+ 20	-700	-1475
After Gel	- 35	-615	-1270	+ 90	-355	- 960
After Cure	-135	-715	-1400	- 5	-500	-1035
Loosen Nuts	+315	-450	-1395	+450	-230	-1110

After removal of the retaining nuts, the liner cracked at the ends.

This led to analysis and reevaluation of the stresses and strains developed during the shrink-fitting process. It was deduced that the compressive hoop stresses developed are uniform throughout the length of the liner. The compressive longitudinal stresses, however, must be non-uniform because of the manner in which they are induced. During cooling, the jacket grabs the liner and drags it along as it attempts to return to its original room temperature dimensions. The success of the jacket depends not only on the shrink pressure but also on the coefficient of friction and the length of the liner that this coefficient must act upon. Therefore in regards to the longitudinal stresses, one would expect a stress pattern which would look like a normal distribution curve. Maximum stress would be at the center of the liner, while minimum stresses would result at the ends, thus the benefit that is received from shrink fitting is not as adequate as expected. Regarding specimen #60-6 the strain gages were mounted at the center of the liner. The compressive strain recorded in gage #4 (-255  $\mu\text{in/in}$ ) would be the maximum. At the ends, however, the strain could be negligible and therefore the tensile strain from winding (+450  $\mu\text{in/in}$ ) might represent the true stresses developed in the liner and this is the reason it cracked at the ends.

A third cylinder (60-7) was fabricated with the .002" radial interference. This cylinder was composed of a .200" wall gun steel (mod. 4337) jacket, shrunk over an alumina liner.

The gun steel jacket has a radially expansion of only  $\sim .0008''/100^\circ\text{F}$  and therefore a  $\Delta T$  of  $\sim 250^\circ\text{F}$  is necessary for a size for size fit. Because of the aforementioned machining tolerances, the shrink fitting was done at an oven temperature of  $675^\circ\text{F}$  ( $600 \Delta T$ ).

Because of the higher shrink-fitting temperature, strain gages were not used to measure the induced strain. Instead a dimensional profile of the liner's I.D. was done before and after shrinking. This data is shown in Table 11.

The steel jacket was selected for fabrication because of its greater elastic modulus over the aluminum material. This, in turn, would induce a larger hoop stress for the same radial interference of  $.002''$ . In addition there is numerous data in the handbooks on the friction coefficient of steel on alumina. The value of  $.3$  for this combination is much more reliable. Table 11 also shows the calculations which correlates the recorded hoop deflections at the center of the liner with strain and stress. These values are then converted into a shrink fitting pressure which is used to find the induced longitudinal stress and strain at the base of the liner.

This specimen was stress analyzed using the X-Ray residual stress analysis. Through a technique developed by G. P. Capsimalis, et al, the state of stress of isotropic materials can be determined quite accurately through x-ray measurements of the lattice strains.

---

<sup>3</sup>G. P. Capsimalis, R. F. Haggerty, K. Loomis, "Computer Controlled X-Ray Stress Analysis for Inspection of Manufactured Components," Watervliet Arsenal Technical Report WVT-TR-77001, January 1977.

TABLE 11. INSIDE DIAMETER PROFILE OF SPECIMEN 60-7 BEFORE AND AFTER SHRINK-FITTING (0 = 2.360")

	12 O'CLOCK			3 O'CLOCK		
	Before	After	$\Delta D_{\text{mils}}$	Before	After	$\Delta D_{\text{mils}}$
1"	-.0020	-.0050	-3.0	-.0020	-.0053	-3.3
2"	-.0017	-.0046	-2.9	-.0020	-.0053	-3.3
3"	-.0014	-.0038	-2.4	-.0018	-.0047	-2.9
4"	-.0011	-.0033	-2.2	-.0018	-.0047	-2.9
5"	-.0010	-.0035	-2.5	-.0018	-.0053	-3.5
6"	-.0010	-.0037	-2.7	-.0020	-.0053	-3.3
7"	-.0014	-.0038	-2.4	-.0022	-.0055	-3.3
8"	-.0016	-.0043	-2.8	-.0023	-.0056	-3.3
9"	-.0010	-.0042	-3.2	-.0020	-.0060	-4.0

In 4, 5, & 6 inch region, ave.  $\Delta D = -3.9$  mils

Comparable Strain:  $D \cdot \epsilon_H$

$$\epsilon_H = -.0029/2.360 = -1228 \text{ } \mu\text{in/in}$$

$$\sigma_H = \epsilon_H \cdot E = (-1229)(55) = -67,585 \text{ Psi}$$

$$P_f = \frac{E\epsilon_H(w^2-1)}{-2w^3} = \frac{(-67,585)(.248)}{-2(1.248)} = 6715$$

$$\text{If } P_f = 6715 \text{ Psi, Axial force} = 2\pi \cdot b \cdot l \cdot P_f \cdot f = 2\pi(1.318)(5)(6715)(.3) = 83,415 \text{ Psi}$$

$$\sigma_L = F/A = 83,415/1.083 = -77,023$$

$$\epsilon_L = \sigma_L/E = -77,023/55 \times 10^6 = 1400 \text{ } \mu\text{in/in}$$

The present limitation of the x-ray equipment allows for residual stress measurements only on outside surfaces. This limited the investigation to the residual stresses in the steel jacket. However, the data developed below is indicative of the end effects mentioned above.

Residual Stresses	Location		
	Left End	Middle	Right End
Longitudinal Stress (Psi)	6,005	32,323	8,179
Hoop Stress (Psi)	24,319	33,572	25,007

The measurements were made in two axial planes 90° apart. The readings at the left and right ends of the specimen were made 1 in. from each end while center readings were at the 5 in. location. These locations are shown as the polished areas of #60-7 shown in Figure 24. The stress data are averages of the longitudinal stresses which were induced into the jacket by the shrink-fitting process.

From the above, it is evident that residual longitudinal stresses exist on the O.D. of the jacket which decrease from a maximum in the center to a minimum at both ends. Although the magnitude will vary, one would expect the same type of normal distribution of longitudinal stresses to occur in the ceramic liner. The longitudinal tensile residual stresses measured in the jacket are related to longitudinal compressive residual stresses which have been set up in the liner by the shrink fitting process. One would therefore conclude that the

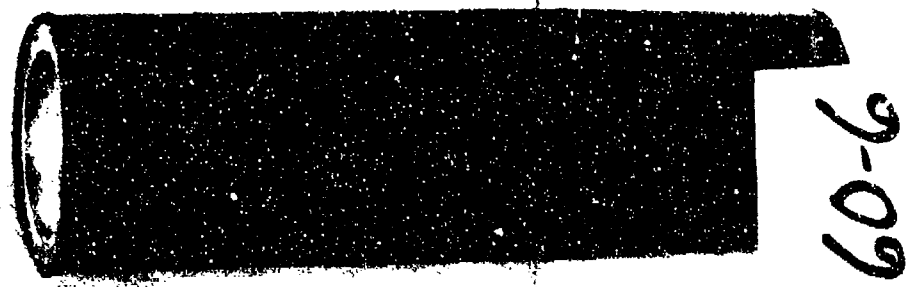
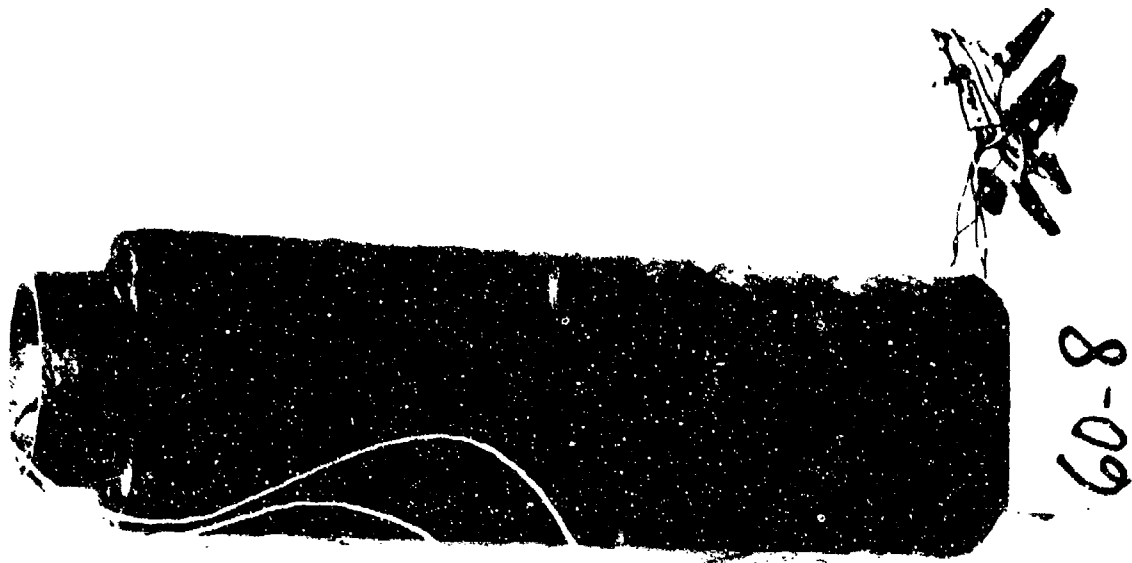


Figure 24. Specimens 60-6, -7, and -8 from Phase III

liner's stresses are maximum at the center and at a minimum at both ends.

A fourth cylinder (#60-8) was fabricated of steel jacket/alumina liner using the same dimensions and procedures as in #60-7. Table 12 shows the I.D. profile of the liner before and after shrinking. This specimen was prepared while specimen #60-7 was in the process of being analyzed. Although the presence of this normal distribution of stresses was anticipated, the large strains induced by the steel jacket might enable a successful overwrap even though they were at a minimum at the ends.

Fifty five hoop layers were wound at a tension of 6 lb/end and a coverage of 162 ends/in/layer. As with all previous windings, the same 6 mil NS-355 wire with anhydride cured epoxy binder was used to fabricate the composite overwrap.

Before winding, three strain gages ( $0^\circ$ ,  $90^\circ$ ) were mounted inside the liner to monitor the hoop and longitudinal strain. Two gages were mounted in the center ( $180^\circ$  apart) and the third gage was mounted 1" from one of the ends. Table 13 shows the strain data recorded during fabrication. This data records the strains induced by the winding operation only. As shown in Table 12, there already were induced compressive residual strains in the liner as a result of the shrink-fitting.

Although the longitudinal tensile strain, from winding, is near the elastic limit for the ceramics, the residual compressive strains before winding reduce the actual longitudinal strains experienced by the liner.

TABLE 12. INSIDE DIAMETER PROFILE OF SPECIMEN 60-8 BEFORE  
AND AFTER SHRINK-FITTING

	<u>12 O'CLOCK</u>			<u>3 O'CLOCK</u>		
	Before	After	$\Delta D_{\text{mils}}$	Before	After	$\Delta D_{\text{mils}}$
0"	+0.0020	-0.0005	-2.5	-0.0011	-0.0010	-2.1
1"	+0.0014	-0.0013	-2.7	+0.0007	-0.0015	-2.2
2"	+0.0010	-0.0015	-2.5	+0.0006	-0.0015	-2.1
3"	+0.0008	-0.0020	-2.8	+0.0005	-0.0018	-2.3
4"	+0.0005	-0.0019	-2.4	+0.0002	-0.0018	-2.0
5"	+0.0002	-0.0020	-2.2	.0000	-0.0025	-2.5
6"	.0000	-0.0026	-2.6	-0.0002	-0.0024	-2.2
7"	-0.0004	-0.0028	-2.4	-0.0003	-0.0025	-2.2
8"	-0.0010	-0.0034	-2.4	-0.0005	-0.0028	-2.3
9"	-0.0014	-0.0039	-2.5	-0.0007	-0.0032	-2.5
10"	-0.0015	-0.0028	-1.8	-0.0005	-0.0019	-1.4

In the 4, 5, & 6 inch region, ave.  $\Delta D = -2.3$  mils

Comparable strain =  $-0.0023/2.360 = -974 \mu\text{in/in}$

$$\sigma_H = \epsilon_H \cdot E = (-974)(50) = -53,570 \text{ Psi}$$

$$P_f = \frac{E\epsilon_H(w^2-1)}{-2w^2} = \frac{(-53,570)(.248)}{-2(1.248)} = 5323$$

$$\text{If } P_f = 5323, \text{ Axial force} = 2\pi \cdot b \cdot l \cdot P_f \cdot f = 2\pi(1.318)(5)(5323)(.3) \\ = 66,117$$

$$\sigma_L = F/A = 66,117/1.083 = 61,050$$

$$\epsilon = \sigma_L/E = 61,050/55 \times 10^6 = -1110 \mu\text{in/in}$$

TABLE 13. INTERNAL STRAIN DATA FROM THE WINDING OF SPECIMEN 60-8

<u>No. of Layers</u>	<u>CENTER</u>				<u>END</u>	
	<u>GAGE #1</u>		<u>GAGE #2</u>		<u>GAGE #3</u>	
	$\epsilon_H$	$\epsilon_L$	$\epsilon_H$	$\epsilon_L$	$\epsilon_H$	$\epsilon_L$
0	0	0	0	0	0	0
Tighten Nuts	0	- 70	0	- 70	0	- 70
1 - 10 Hoops	- 600	+ 85	- 590	+ 70	- 600	+ 80
11 - 20 Hoops	-1140	+240	-1120	+220	-1125	+230
21 - 25 Hoops	-1355	+305	-1365	+285	-1370	+290
After Gel	-1050	+255	-1000	+180	-1200	+ 50
26 - 35 Hoops	-1495	+425	-1480	+340	-1630	+255
36 - 45 Hoops	-1950	+580	-1925	+505	-2060	+445
46 - 55 Hoops	-2350	+755	-2340	+675	-2470	+620
After Gel	-2015	+670	-2060	+575	-2235	+415
1 & 2 Helical	-1975	+580	-2150	+460	-2230	+440
After Cure	-2080	+555	-2140	+475	-2355	+300
Loosen Nuts	-2115	+680	-2195	+590	-2385	+460

This is true at the ends of the cylinder which were the areas of most concern. No liner cracks were found when inspected with the liquid dye penetrant. Reinspection one week later however, did show evidence of circumferential cracks in the ceramic liner.

#### PHASE IV

Phases I through III show that for the ceramic liner to be useful in gun tube applications, it must be preloaded axially under all operating conditions.

Phase IV investigates the feasibility of inducing longitudinal compressive stresses in the 60 mm ceramic liner by shrink fitting alone. These compressive stresses, as shown in Figure 25, are originated by friction during the cooling process and they increase linearly toward the center of the liner as stated in Phase III. Their magnitude is a function of the component's geometry, the coefficient of friction, and the normal pressure induced by the mechanical interference employed.

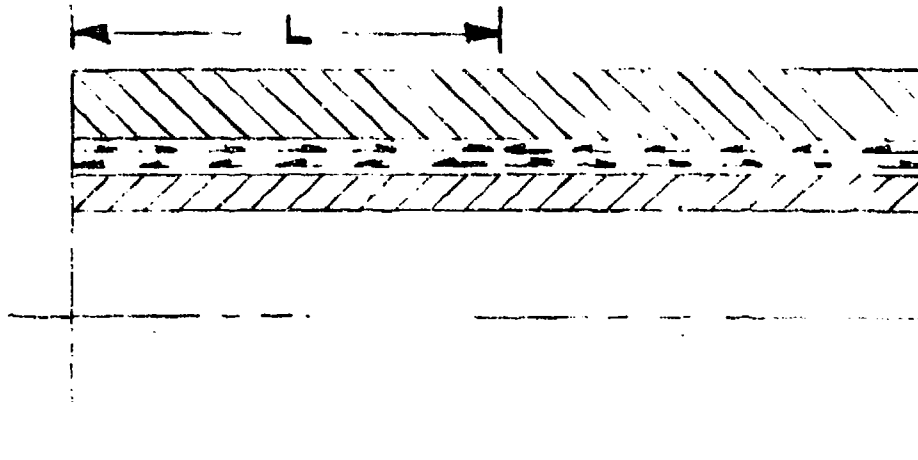


Figure 25. Schematic showing action of friction forces

In an equation form, the axial force that a shrink-fit assembly can stand without separation of the components is:

$$F = 2\pi bL P_f f$$

where  $F$  is the force;  $L$  is half the length of the assembly,  $P_f$  is the shrink-fit pressure, and  $f$  is the coefficient of friction.

Figures 26 and 27 which are outputs from computer program SHIFUTMP show the radial and tangential residual stress distributions caused by a radial mechanical interference of 0.002 inches. Note that  $P_b$  from Figure 26 is approximately  $-4.2 \times 10^3$  Psi while Figure 27 shows the ceramic liner with a compressive stress of  $3.5 \times 10^4$  Psi at the bore, and the steel jacket with a tensile stress of  $2.6 \times 10^4$  Psi at the interface. Figures 28 and 29 show the stress distributions, in the same geometry of Figures 26 and 27, produced by an internal pressure of 12,000 Psi. At this pressure the ceramic liner is near its tensile strength capacity of approximately 35,000 Psi.

The design of any one gun section depends on the conditions imposed on it, and must be treated accordingly. Assuming that yielding shall occur simultaneously in all of the component tubes, what will be the necessary shrinkages, considering the component strengths, elastic constants, etc.?

Table 14, showing a computer printout for this case, suggests that for the same aforementioned gun tube geometry the 12,000 Psi pressure can be boosted to 24,881 Psi if a mechanical radial interference of 0.0061" were imposed.

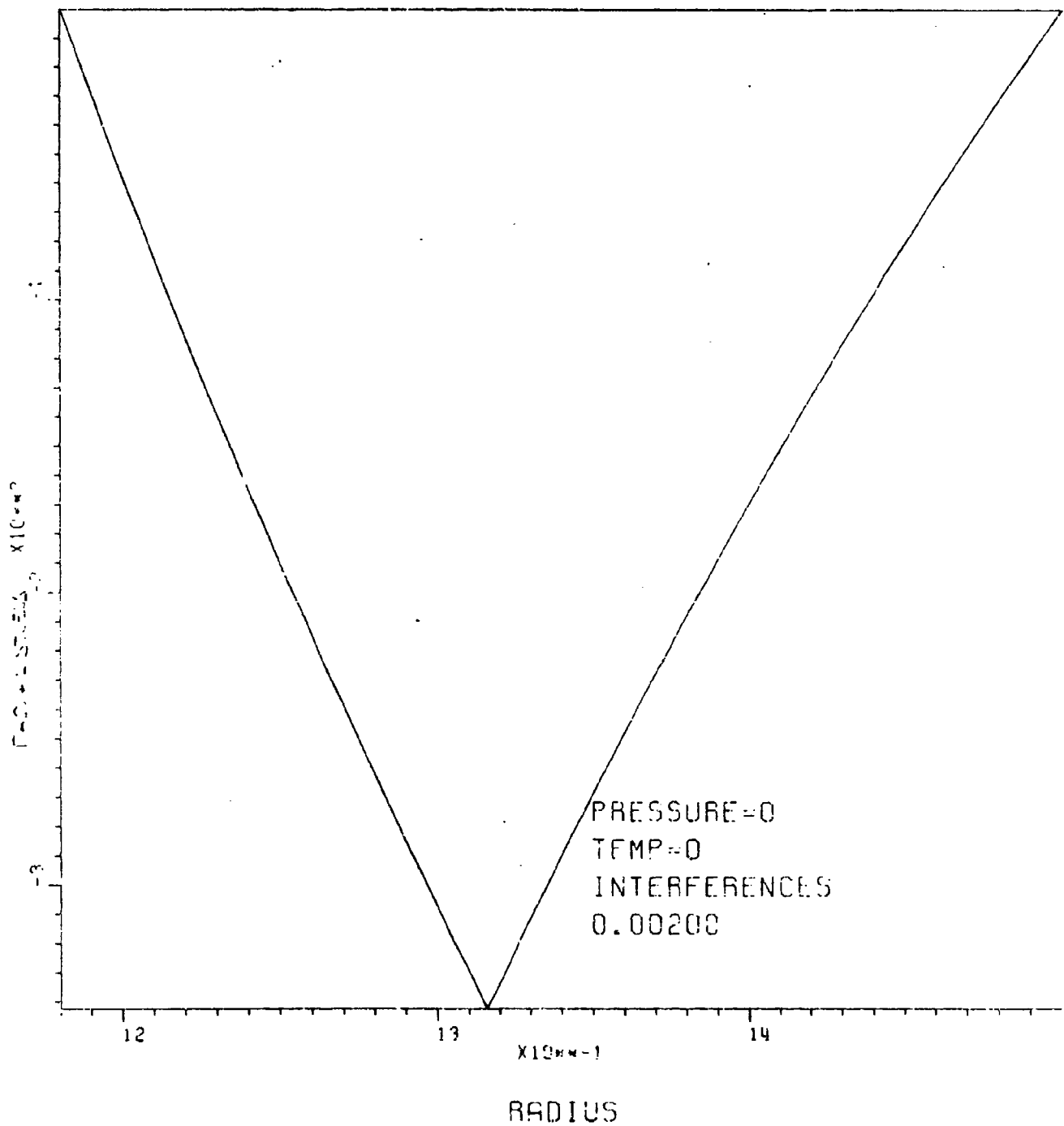


Figure 26. Radial stress distribution caused by .002" interference fit

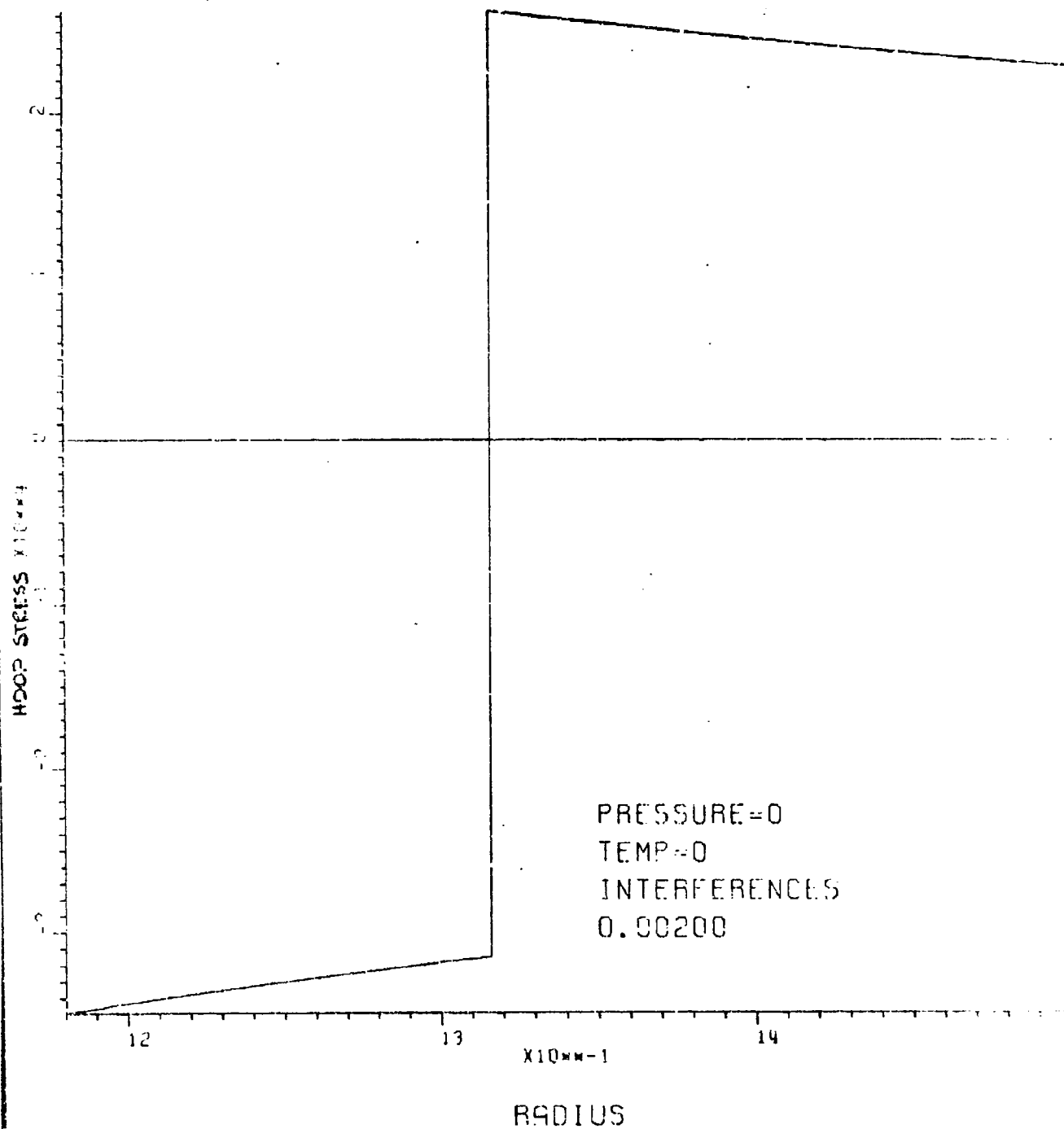


Figure 27. Tangential stress distribution caused by .002" interference fit

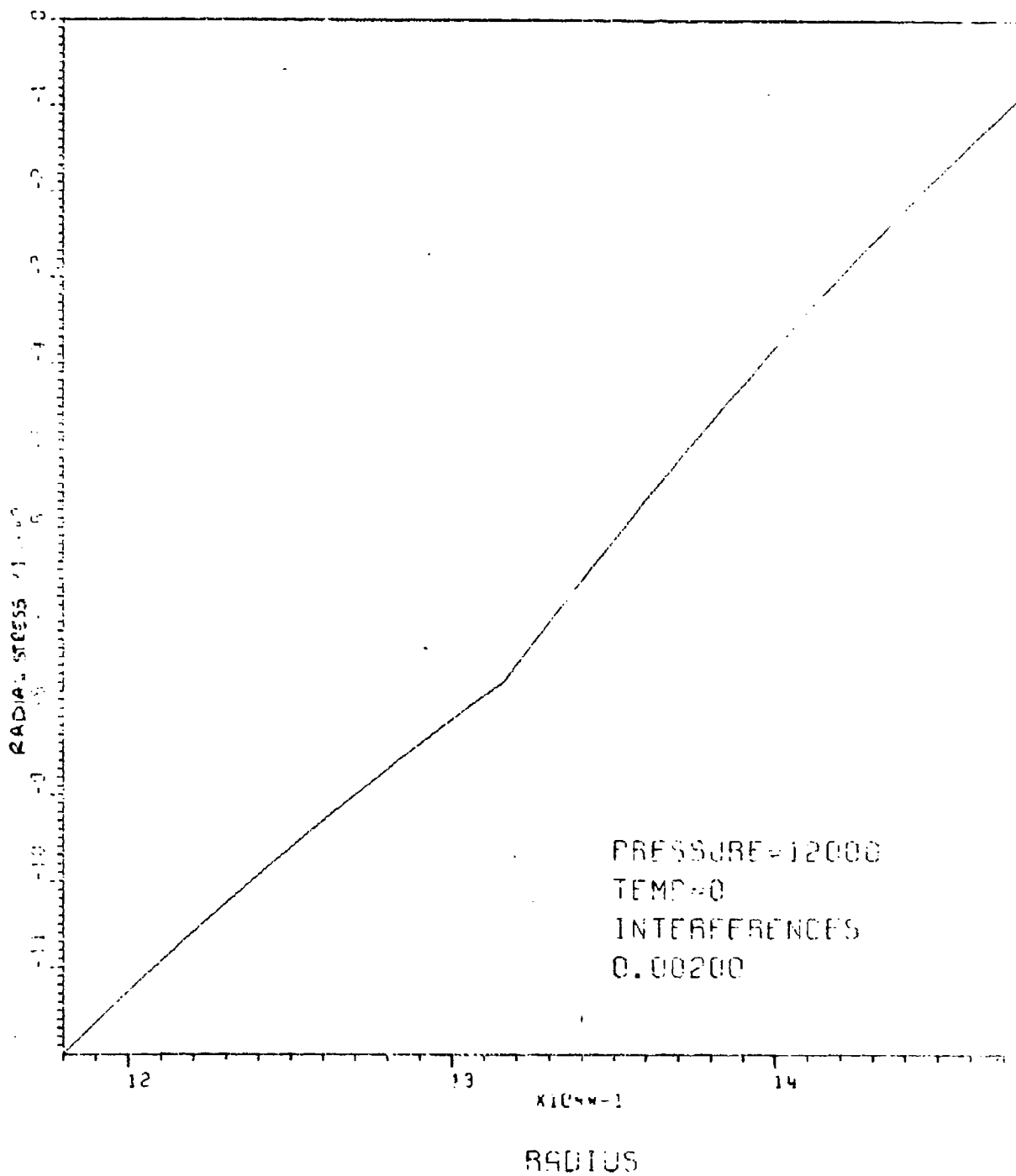


Figure 38. Radial stress distribution caused by 12 Ksi internal pressure

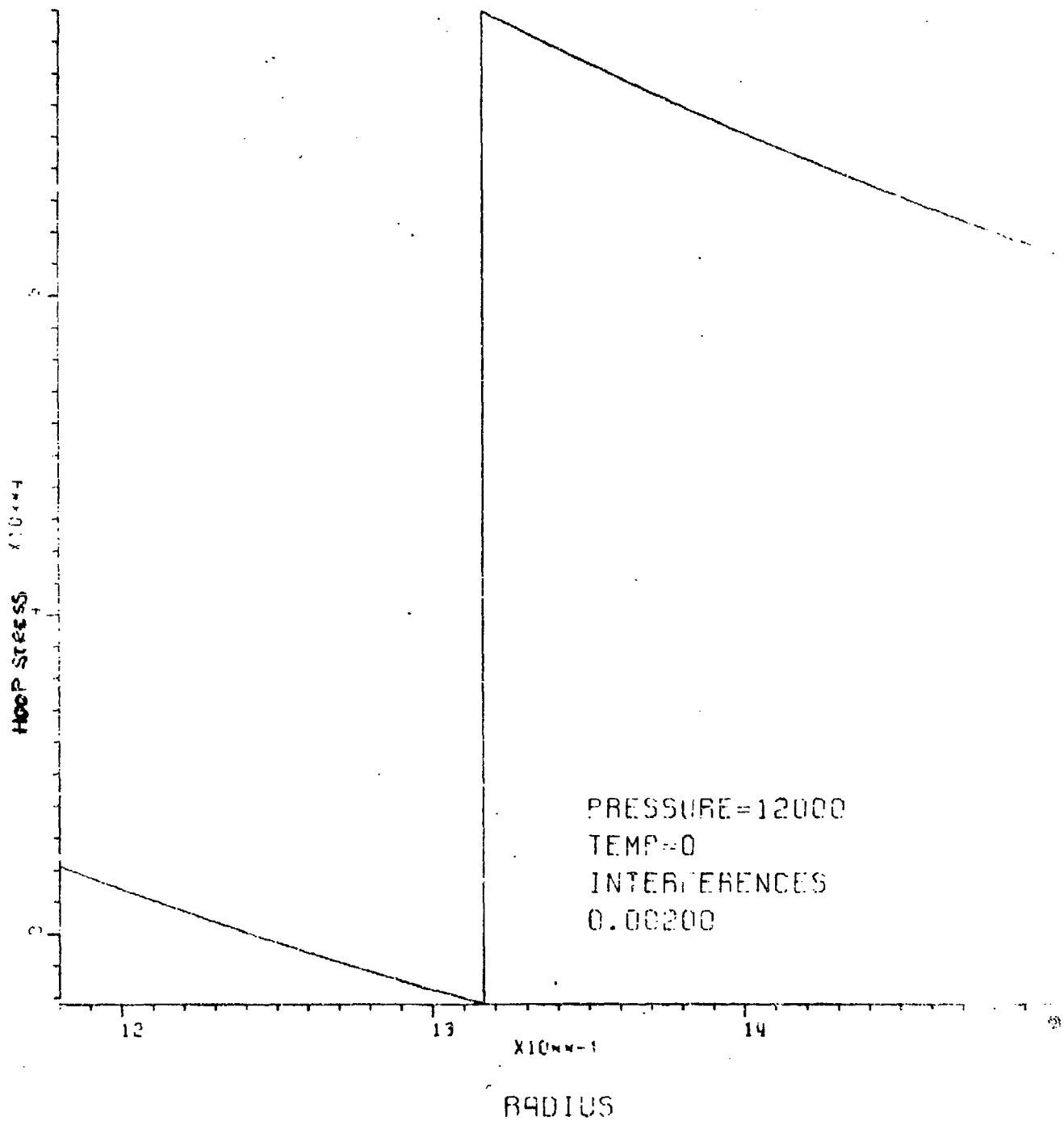


Figure 29. Tangential stress distribution caused by 12 Ksi internal pressure

Although this concept seems to give a possible solution, it cannot be optimized since, at the cylinder's ends, the axial holding force is negligible; recall that this force increases linearly toward the center of the liner.

An attempt was made to verify the theory presented above. The outcome was doubtful at the start because of the thermal shock limitation of the ceramic material. The vendor's literature, and subsequent telecons with their engineering personnel, indicated that the maximum  $\Delta T$  shock that the Alumina would withstand was 1000°F.

In order to induce a .006" radial interference fit with a gun steel jacket, it was necessary to heat the jacket above 830°F. This temperature provides the proper  $\Delta T$  for a size for size fit of jacket over liner.

Recognizing the aforementioned dimensional machining tolerances of both the liner and jacket it was necessary to heat the jacket above this 830°F temperature. Since the inside radius of the jacket increases at a rate of .0008"/100°F( $\Delta T$ ), it was necessary to heat the jacket to at least 1100°F to allow for the proper insertion of the ceramic liner into the jacket. This jacket temperature results in a thermal shock of ~ 1000°F experienced by the ceramic liner, which approaches the maximum  $\Delta T$  that the material is "claimed" to be able to withstand.

TABLE 14. COMPUTER PRINTOUT DATA ON SIMULTANEOUS LINER/JACKET  
YIELDING (SHFUTMP)

No. of Cylinders = 2

- Cylinder (Ceramic) 1
  - R(Inner) = 1.1800 R(Outer) = 1.3180
  - Young's Modulus = 55000000
  - Poisson's Ratio = 0.200
  - Yield Strength = 30000
- Cylinder 2
  - R(Inner) = 1.3180 R(Outer) = 1.5000
  - Young's Modulus = 30000000
  - Poisson's Ratio = 0.300
  - Yield Strength = 160000
- Simultaneous Yielding of All Cylinders
  - Relative Position of Yield = 0.0
  - Stresses at Yield Point, SIGR = -0.1923236E 05 SIGTH = 0.1495139E 06
  - Von Mises' Criterion = 0.1599994E 06
  - Inner Pressure = 0.1923248E 05
  - Inner Stresses, R = 1.3180
    - SIGR = -0.1923236E 05
    - SIGTH = 0.1495139E 06
  - Outer Stresses, R = 1.5000
    - SIGR = 0.9139627E-01
    - SIGTH = 0.1302815E 06

TABLE 14. COMPUTER PRINTOUT DATA ON SIMULTANEOUS LINER/JACKET  
YIELDING (SHFUTMP)(CONT)

Cylinder 1

Relative Position of Yield = 0.0

Stresses at Yield Point, SIGR = -0.2465557E 05 SIGTH = 0.2999980E 05

Ceramic Material

Relative Position of Yield = 0.0

Stresses at Yield Point, SIGR = -0.2488310E 05 SIGTH = 0.2999979E 05

Ceramic Material

Relative Position of Yield = 0.0

Stresses at Yield Point, SIGR = -0.2488158E 05 SIGTH = 0.2999979E 05

Ceramic Material

• Inner Pressure = 0.2488160E 05

Inner Stresses, R = 1.1800

SIGR = -0.2488158E 05  
SIGTH = 0.2999979E 05

Outer Stresses, R = 1.3241

SIGR = -0.1923246E 05  
SIGTH = 0.2435067E 05

• Cylinder 1

R(Inner) = 1.1800 R(Outer) = 1.3241

Interference = 0.0061

Cylinder 2

R(Inner) = 1.3180 R(Outer) = 1.5000

TABLE 14. COMPUTER PRINTOUT DATA ON SIMULTANEOUS LINER/JACKET  
YIELDING (SHFUTMP) (CONT)

• Residual Stresses

Cylinder 1

Inner Stresses, R = 1.1800

SIGR = -0.2164384E-01

SIGTH = -0.1066333# 06

Outer Stresses, R = 1.3241

SIGR = -0.1097613E 05

SIGTH = -0.9565713E 05

Cylinder 2

Inner Stresses, R = 1.3180

SIGR = -0.1097609E 05

SIGTH = 0.8532875E 05

Outer Stresses, R = 1.5000

SIGR = 0.2284907E-01

SIGTH = 0.7435269E 05

Two attempts were made to shrink fit at this temperature and, on both occasions the liners, although successfully inserted into the liners, cracked within a minute of insertion. A final attempt was made at a jacket temperature of 900°F, however, this temperature did not allow for the complete insertion of the liner. It "hung up" about 1/3 of the way through the jacket.

No further attempts were made to shrink fit the steel jacket/alumina liner to the .006" radial interference. This phase was discontinued because of the limitations imposed by the physical and mechanical properties of the two materials.

#### SUMMARY

A theoretical analysis predicting the state of stress in refractory-lined composite gun barrels has been developed and tested. The prominent problem in fabricating such barrels has been to restrict the ceramic liner from going into tension in the axial direction during the application of residual hoop stress, and simultaneously to have sufficient residual longitudinal tensile strength to accommodate the longitudinal firing stresses. Recalling that the ceramic used has a tensile yielding strength of approximately 30 Ksi and a modulus of elasticity of 55 and  $10^6$  Psi, one can determine the maximum longitudinal strain,  $\epsilon_z$ , that the ceramic can withstand is - 550  $\mu\text{in/in}$ . The  $\epsilon_z$  is related to the outside pressure, P, exerted on the liner by

$$\epsilon_z = \frac{.6 P_0 w^2}{E(w^2-1)} \quad (1)$$

and the hoop stress generated, at the bore, by the same  $P_o$  is given by

$$\sigma_H = - \frac{2 P_o w^2}{w^2 - 1} \quad (2)$$

From (1) and (2), one can conclude that the  $\sigma_H$  at the bore must be less than -100 Ksi even though the ceramic can take up to 350 Ksi in compression.

From this introduction, and (2), it can be seen (Figure 30) that if  $\sigma_H$  is fixed at -100 Ksi a limiting value for  $P_o$  can be obtained for a specific liner wall ratio,  $w$ .

Figure 30 shows that for the 60 mm ceramic liner the outside pressure exerted on the liner by the filament winding, shrink fitting process, or combination of the two, should not exceed 12 Ksi. On the other hand, in order to make use of the high compressive strength of the ceramic (-350 Ksi), the  $P_o$  needed is approximately 35 Ksi for a  $w$  of 1.117 (from Eq. 2). To apply this  $P_o$ , one must either:

a. Restrain the cylinder's ends - this was accomplished by mechanical straining devices, helical wrapping of the liner, and compressive stresses induced during the cooling of a metallic sleeve shrink fitted over the ceramic liner. Although the latter one seems to give a possible solution it cannot be optimized at the cylinder's ends since the axial holding force increases linearly toward the center of the liner. Perhaps a combination of the three concepts would give a possible solution.

Po

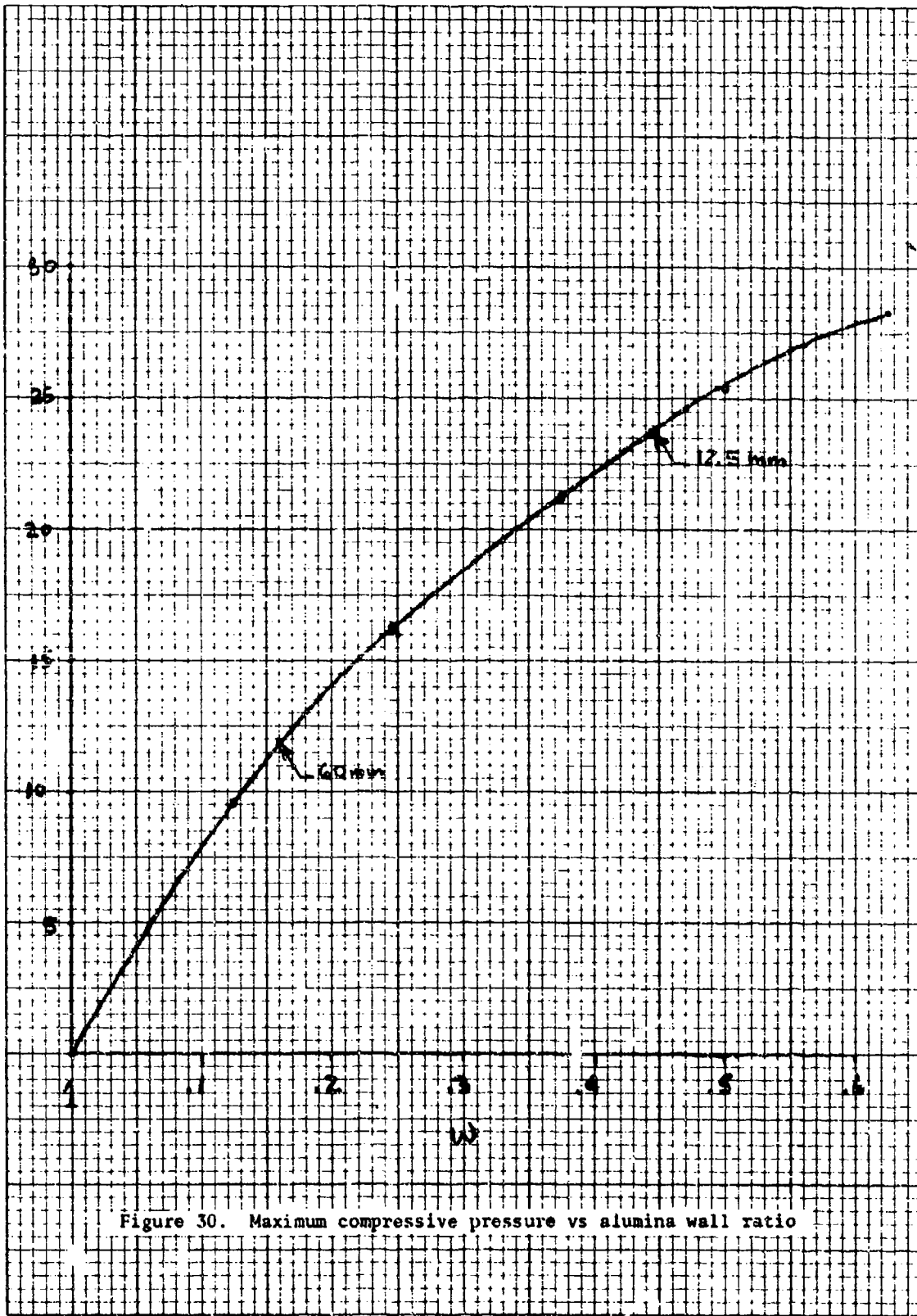


Figure 30. Maximum compressive pressure vs alumina wall ratio

b. Increase the wall thickness of the liner - this idea, although interesting, was disregarded since (1) for large bore diameters, as explained by the ceramic manufacturers, the wall thickness cannot exceed ~ .15" for a homogeneous, isotropic structure, and (2) the curve of Figure 30 does not offer any reasonable wall ratio for a 35 Ksi outside pressure.

Table 5 of this report shows strain gage data obtained from specimen 60-1. This specimen was not restricted longitudinally and it failed upon the application of the 19th layer. Note that after the 18th layer, the 45° Rosette reported an average hoop strain,  $\epsilon_H$ , of -2000  $\mu\text{in/in}$ , and an average longitudinal strain of +482  $\mu\text{in/in}$ . From Hooke's Law ( $\sigma = E\epsilon$ ),  $\sigma_H$  becomes -110 Ksi or from Eq. (2)  $P_0$  is calculated to be ~ 12 Ksi: the same value predicted by the theory in Figure 30.

#### CONCLUSIONS

This investigation has revealed serious technological problems associated with the use of large ceramic liners in cannon barrels. Among these problems are the great difficulty in controlling longitudinal residual stresses, the controlling of dimensional tolerances over reasonable liner length, the thermal gradients at the instant of contact of the components, the effects of shrinkage temperature over 500°F on sleeve material and, finally, other possible problems associated with the riflings of ceramic.

Although the design methodology has been developed and shows good correlation with the experimental results on the larger diameter ratio 12.5 mm specimens, larger diameter specimens with smaller diameter ratio configurations are limited by the low tensile fracture strength of the material.

The limited work on the 6.4 mm tungsten-carbon alloy liners did not present any of the aforementioned problems encountered with the ceramic liners (this of course, is attributed to their high compressive and tensile strength values), however, because the current commercial requirements include only the manufacturing of tubing up to 12" long and 0.125" diameter, further work has been discontinued.

#### REFERENCES

1. L. A. Behrman, et al., "Feasibility of Refractory-Lined Composite Gun Barrels," Physics International Co. Report No. PIIR-11-72, February 1972.
2. G. D'Andrea and R. Cullinan, "Application of Filament Winding to Cannon and Cannon Components. Part III: Summary," Watervliet Arsenal Technical Report WVT-TR-76035, October 1976.
3. G. P. Capsimalis, R. F. Haggerty, K. Loomis, "Computer Controlled X-Ray Stress Analysis for Inspection of Manufactured Components," Watervliet Arsenal Technical Report WVT-TR-77001, January 1977.

EXTERNAL DISTRIBUTION LIST

	<u>NO. OF COPIES</u>		<u>NO. OF COPIES</u>
ASST SEC OF THE ARMY RESEARCH & DEVELOPMENT ATTN: DEP FOR SCI & TECH THE PENTAGON WASHINGTON, D.C. 20315	1	COMMANDER US ARMY TANK-AUTMV R&D COMD ATTN: TECH LIB - DRDTA-UL MAT LAB - DRDTA-RK WARREN, MICHIGAN 48090	1 1
COMMANDER US ARMY MAT DEV & READ. COMD ATTN: DRCDE 5601 EISENHOWER AVE ALEXANDRIA, VA 22333	1	COMMANDER US MILITARY ACADEMY ATTN: CHMN, MECH ENGR DEPT WEST POINT, NY 10996	1
COMMANDER US ARMY ARRADCOM ATTN: DRDAR-TSS DRDAR-LCA (PLASTICS TECH EVAL CEN) DOVER, NJ 07801	2 1	COMMANDER REDSTONE ARSENAL ATTN: DRSMI-RB DRSMI-RPS DRSMI-RSM ALABAMA 35809	2 1 1
COMMANDER US ARMY ARRCOM ATTN: DR SAR-LEV-1 ROCK ISLAND ARSENAL ROCK ISLAND, IL 61299	1	COMMANDER ROCK ISLAND ARSENAL ATTN: SARRI-ENM (MAT SCI DIV) ROCK ISLAND, IL 61202	1
DIRECTOR JS Army Ballistic Research Laboratory ATTN: DRDAR-TSB-S (STINFO) ABERDEEN PROVING GROUND, MD 21005	1	COMMANDER HQ. US ARMY AVN SCH ATTN: OFC OF THE LIBPARIAN FT RUCKER, ALABAMA 36362	1
COMMANDER US ARMY ELECTRONICS COMD ATTN: TECH LIB FT MONMOUTH, NJ 07703	1	COMMANDER US ARMY FGN SCIENCE & TECH CEN ATTN: DRXST-SD 220 7TH STREET, N.E. CHARLOTTESVILLE, VA 22901	1
COMMANDER US ARMY MOBILITY EQUIP R&D COMD ATTN: TECH LIB FT BELVOIR, VA 22060	1	COMMANDER US ARMY MATERIALS & MECHANICS RESEARCH CENTER ATTN: TECH LIB - DPXMR-PL WATERTOWN, MASS 02172	2

NOTE: PLEASE NOTIFY COMMANDER, ARRADCOM, ATTN: BENET WEAPONS LABORATORY,  
DRLAR-LCB-TL, WATERVLIET ARSENAL, WATERVLIET, N.Y. 12189, OF ANY  
REQUIRED CHANGES.

EXTERNAL DISTRIBUTION LIST (CONT)

	<u>NO. OF COPIES</u>		<u>NO. OF COPIES</u>
COMMANDER US ARMY RESEARCH OFFICE P.O. BOX 12211 RESEARCH TRIANGLE PARK, NC 27709	1	COMMANDER DEFENSE DOCU CEN ATTN: DDC-TCA CAMERON STATION ALEXANDRIA, VA 22314	12
COMMANDER US ARMY HARRY DIAMOND LAB ATTN: TECH LIB 2800 POWDER MILL ROAD ADELPHIA, MD 20783	1	METALS & CERAMICS INFO CEN BATTELLE COLUMBUS LAB 505 KING AVE COLUMBUS, OHIO 43201	1
DIRECTOR US ARMY INDUSTRIAL BASE ENG ACT ATTN: DRXPE-MT ROCK ISLAND, IL 61201	1	MPDC 13919 W. BAY SHORE DR. TRAVERSE CITY, MI 49684	1
CHIEF, MATERIALS BRANCH US ARMY R&S GROUP, EUR BOX 65, FPO N.Y. 09510	1		
COMMANDER NAVAL SURFACE WEAPONS CEN ATTN: CHIEF, MAT SCIENCE DIV DAHLGREN, VA 22448	1		
DIRECTOR US NAVAL RESEARCH LAB ATTN: DIR, MECH DIV CODE 26-27 (DOC LIB) WASHINGTON, D.C. 20375	1 1		
NASA SCIENTIFIC & TECH INFO FAC P.O. BOX 8757, ATTN: ACQ BR BALTIMORE/WASHINGTON INTL AIRPORT MARYLAND 21240	1		

NOTE: PLEASE NOTIFY COMMANDER, ARRADCOM, ATTN: BENET WEAPONS LABORATORY,  
DRDAR-LCB-TL, WATERVLIET ARSENAL, WATERVLIET, N.Y. 12189, OF ANY  
REQUIRED CHANGES.

WATERVLIET ARSENAL INTERNAL DISTRIBUTION LIST

	<u>NO. OF COPIES</u>
COMMANDER	1
DIRECTOR, BENET WEAPONS LABORATORY	1
CHIEF, DEVELOPMENT ENGINEERING BRANCH	1
ATTN: DRDAR-LCB-DA	1
-DM	1
-DP	1
-DR	1
-DS	1
-DC	1
CHIEF, ENGINEERING SUPPORT BRANCH	1
CHIEF, RESEARCH BRANCH	2
ATTN: DRDAR-LCB-RA	1
-RC	1
-RM	1
-RP	1
TECHNICAL LIBRARY	5
TECHNICAL PUBLICATIONS & EDITING UNIT	2
DIRECTOR, OPERATIONS DIRECTORATE	1
DIRECTOR, PROCUREMENT DIRECTORATE	1
DIRECTOR, PRODUCT ASSURANCE DIRECTORATE	1

NOTE: PLEASE NOTIFY DIRECTOR, BENET WEAPONS LABORATORY, ATTN:  
DRDAR-LCB-TL, OF ANY REQUIRED CHANGES.